Supporting Information

Asymmetric Trifluoromethylthiolation of Azlactones under Chiral Phase Transfer Catalysis

Marina Sicignano,[a] Ricardo I. Rodríguez,[b] Vito Capaccio,[b] Fabio Borello,[a] Rafael Cano,[b] Francesco De Riccardis,[a] Luca Bernardi,[c] Sergio Díaz-Tendero,[d] Giorgio Della Sala[a,*] and José Alemán[b,*]

gdsala@unisa.it; jose.aleman@uam.es

[a] *Dipartimento di Chimica e Biologia "A. Zambelli", Università degli Studi di Salerno, Via Giovanni Paolo II 132, 84084 Fisciano, SA, Italy,*

[b] *Organic Chemistry Department, Módulo 1, Universidad Autónoma de Madrid, 28049 Madrid, Spain.*

[c] *Department of Industrial Chemistry ''Toso Montanari'' & INSTM RU Bologna, Alma Mater Studiorum University of Bologna, Viale del Risorgimento 4, 40136 Bologna, Italy.*

[d] *Chemistry Department, Módulo 13, Universidad Autónoma de Madrid, 28049 Madrid, Spain.*

CONTENTS

General information

All chemicals and solvents were purchased from commercial suppliers and used without further purification. *N*-(trifluoromethylthio)phthalimide **2** was prepared according the reported procedure.[1] Catalysts **I-XXV**, **XXVIII-XXX**[2] and catalysts **XXVI**, **XXVII**[3] were prepared following the general procedure described in the literature.[2] Reactions were monitored by analytical thin layer chromatography (TLC) on precoated silica gel plates (0.25 mm) and visualized by UV light. Flash chromatography was performed on Silica Gel 60 (particle size: 0.040–0.063 mm). ^{1}H-, ^{13}C- and ^{19}F- NMR spectra were recorded on a Bruker Avance III 300 MHz spectrometer and a Bruker Avance-400 spectrometer at room temperature in $CDCl_3$. All NMR spectra were referenced to residual $CHCl_3$ (7.26 ppm, ^{1}H; 77.16 ppm, ^{13}C). The following abbreviations are used to indicate the multiplicity in NMR spectra: s = singlet; d = doublet; dd = double doublet; t = triplet; q = quartet; m = multiplet. Coupling constants (*J*) are quoted in Hertz. Optical rotations were measured on a Perkin-Elmer 241 MC Polarimeter in 10 cm path length cells and are reported as follows: $[\boldsymbol{\alpha}]_{\boldsymbol{D}}^{\boldsymbol{T}}$= (c in g/100 mL, solvent). High resolution mass spectra (HRMS) were acquired using an *Agilent Technologies 6120 Quadrupole LC/MS*, and *MassWorks* software ver. 4.0.0.0 (Cerno Bioscience) was used for the formula identification. *MassWorks* is a MS calibration software which calibrates for isotope profile as well as for mass accuracy allowing highly accurate comparisons between calibrated and theoretical spectra. The samples were ionized in positive ion mode using a ESI ion source. Enantiomeric ratios were determined by chiral HPLC or by Supercritical Fluid Chromatography (SFC) using CHIRALPAK® AS-H (250 x 4.6 mm, 5 µm) and IB (250 x 4.6 mm, 5 µm) columns.

Synthesis azlactones 1a-o

The azlactones **1a-o** were prepared in two steps, slightly modifying synthetic procedures reported in the literature.

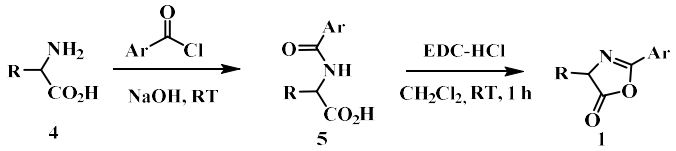

STEP 1.[4] To a solution of amino acid **4** (1.0 eq., 15.0 mmol) in 2 M NaOH aqueous solution (18 ml), aroyl chloride was added (1.0 eq., 15.0 mmol). The resulting reaction mixture was stirred at room temperature until complete homogenization and then acidified to pH 2 by adding 1 M HCl aqueous solution. After 2 hours, the mixture was extracted with EtOAc (2 x 50 ml) and the combined organic phases were dried over Na_2SO_4 and concentrated under reduced pressure. The crude residue **5** was used in the next step without further purification.

STEP 2.[5] *N*-aroyl amino acid **5** (1 eq., 15 mmol) and EDC (1.3 eq., 19.5 mmol) were dissolved in anhydrous CH_2Cl_2 (50 ml) under nitrogen atmosphere. The resulting reaction mixture was stirred at room temperature for 1 hour. The mixture was diluted with additional 50 ml of CH_2Cl_2 and washed with water (2 x 50 ml) and brine solution (30 ml). Then, the organic phase was dried over Na_2SO_4 and concentrated under reduced pressure. In all cases products were obtained in a form suitable for use without further purification.

The characterization data of the compound **1a-e, 1g, 1h, 1j-l** and **1n-o** matched those previously reported.[6] Characterization data of unknown azlactones **1f**, **1i** and **1m** are reported below.

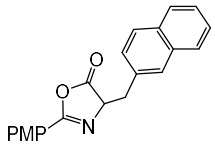

2-(4-methoxyphenyl)-4-(naphthalen-2-ylmethyl)oxazol-5(4*H*)-one (1f): Obtained as a yellow solid (4.6 g, 92% yield), mp 116-117 °C. ^{1}H NMR (300 MHz, $CDCl_3$) δ 7.87 (d, J = 8.8 Hz, 2H), 7.83–7.71 (m, 4H), 7.51–7.37 (m, 3H), 6.90 (d, J = 8.8 Hz, 2H), 4.75 (dd, J = 6.8, 4.9 Hz, 1H), 3.78 (s, 3H), 3.53 (dd, J = 14.0, 4.9 Hz, 1H), 3.33 (dd, J = 14.0, 6.8 Hz, 1H). ^{13}C NMR (75 MHz, $CDCl_3$) δ 177.9, 163.2, 161.5, 133.4, 133.3, 132.6, 129.8, 128.4, 128.0, 127.8, 127.8, 127.7, 126.1, 125.8, 118.1, 114.2, 66.6, 55.4, 37.6. HRMS (ESI) [M + H$^+$] calcd for $C_{21}H_{18}NO_3^+$ 332.1281, found 332.1286.

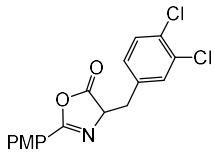

4-(3,4-dichlorobenzyl)-2-(4-methoxyphenyl)oxazol-5(4*H*)-one (1i): Obtained as a yellow solid (4.6 g, 90% yield), mp 108-109 °C. ^{1}H NMR (300 MHz, $CDCl_3$) δ 7.84 (d, J = 8.8 Hz, 2H), 7.36 (d, J = 1.7 Hz, 1H), 7.30 (d, J = 8.2 Hz, 1H), 7.09 (dd, J = 8.2, 1.7 Hz, 1H), 6.92 (d, J = 8.8 Hz, 2H), 4.60 (dd, J = 6.8, 5.0 Hz, 1H), 3.83 (s, 3H), 3.28 (dd, J = 14.1, 5.0 Hz, 1H), 3.07 (dd, J = 14.1, 6.8 Hz, 1H). ^{13}C NMR (75 MHz, $CDCl_3$) δ 177.3, 163.4, 161.8, 135.8, 132.3, 131.6, 131.3, 130.3, 129.8, 129.0, 117.7, 114.3, 65.9, 55.5, 36.4. HRMS (ESI) [M + H$^+$] calcd for $C_{17}H_{14}Cl_2NO_3^+$ 350.0345, found 350.0349.

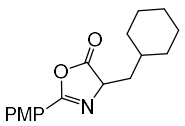

4-(cyclohexylmethyl)-2-(4-methoxyphenyl)oxazol-5(4*H*)-one (1m): Obtained as a white solid (3.6 g, 84% yield), mp 115-114 °C. ^{1}H NMR (300 MHz, $CDCl_3$) δ 7.92 (d, J = 8.9 Hz, 2H), 6.96 (d, J = 8.9 Hz, 2H), 4.41 (dd, J = 8.6, 5.5 Hz, 1H), 3.86 (s, 3H), 1.93 – 1.54 (m, 8H), 1.39–1.10 (m, 3H), 1.07–0.85 (m, 2H). ^{13}C NMR (75 MHz, $CDCl_3$) δ 179.3, 163.1, 161.2, 129.8, 118.3, 114.2, 63.2, 55.5, 39.6, 34.3, 33.5, 32.7, 26.4, 26.1, 26.0. HRMS (ESI) [M + H$^+$] calcd for $C_{17}H_{12}NO_3^+$ 288.1594, found 288.1591.

Typical procedure for the synthesis of racemic compound 3e

In a 4 ml vial, to a mixture of azlactone **1e** (1.0 eq., 0.10 mmol, 28.1 mg), *N*-(trifluoromethylthio)phthalimide **2** (1.2 eq., 0.12 mmol, 29.7 mg), TBAB (0.20 eq., 0.02 mmol, 6.4 mg), and K_3PO_4 (0.1 eq., 0.01 mmol, 2.1 mg) dichloromethane (1.0 mL) was added and the reaction mixture was stirred for 1 hour at -20 °C. Then, the mixture was filtered and concentrated *in vacuo*. The crude residue was purified by chromatography (10 g silica gel cyclohexane-ethyl acetate, 99/1 to 80/20) to afford the desired product **3e** (30.5 mg, 80 % yield) as a white solid.

General procedure for the enantioselective trifluoromethylthiolation of azlactones

In a 4 ml vial, to a mixture of the selected azlactone (1.0 eq., 0.10 mmol), *N*-(trifluoromethylthio)phthalimide **2** (1.2 eq., 0.12 mmol, 29.7 mg), catalyst **VIII** (0.20 eq., 0.02 mmol, 12.6 mg), and K_3PO_4 (0.1 eq., 0.01 mmol, 2.1 mg) dichloromethane (1.0 mL) was added and the reaction mixture was stirred for the indicated time at -20 °C. Then, the mixture was filtered and concentrated *in vacuo*. The crude residue was purified by chromatography (10 g silica gel cyclohexane-ethyl acetate, 99/1 to 80/20) to afford the corresponding product.

Optimization of reaction conditions

Base screening of asymmetric trifluoromethylthiolation of 1a

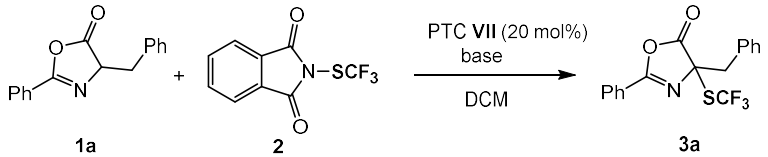

1a 2 3a

entry	Base	T (°C)	t (h)	yield (%)[a]	er[b]
1	K_3PO_4 (aq.) 10%	RT	16	28	64:36
2	K_3PO_4 (s) 5.0 eq.	RT	1	42	57:43
3	K_3PO_4 (s) 5.0 eq.	0	2	45	59:41
4	K_3PO_4 (s) 0.1 eq.	RT	5	64	65:35
5	K_3PO_4 (s) 0.1 eq.	-20	65	74	72:28
6	K_3PO_4 (s) 0.1 eq.	-40	65	35	62:38

[a] Isolated yield. [b] Determined by HPLC on a chiral stationary phase.

Catalyst screening for asymmetric trifluoromethylthiolation of 1a

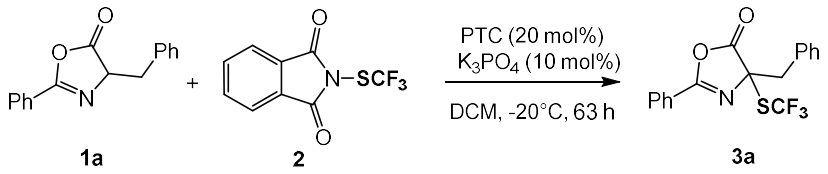

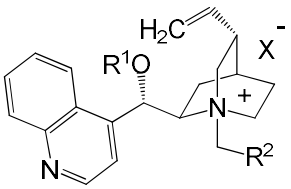

I R^1= allyl; R^2= Ph; X= Br **3a:** 80%y; 51:49er
II R^1= benzyl; R^2= Ph; X= Br **3a:** 86%y; 52:48er
III R^1= 1-adamanthyl; R^2= Ph; X= Br **3a:** 72%y; 51:49er
IV R^1= H; R^2= Ph ; X= Br **3a:** 91%y; 72:28er
V R^1= H; R^2= 4-OMe-Ph ; X= Br **3a:** 78%y; 53:47er
VI R^1= H; R^2= 4-NO_2-Ph ; X= Br **3a:** 57%y; 77:23er
VII R^1= H; R^2= 3,5-$(CF_3)_2$-Ph ; X= Br **3a:** 74%y; 72:28er
IX R^1= H; R^2= 4-Cl-Ph ; X= Br **3a:** 57%y; 75:25er
X R^1= H; R^2= 4-F-Ph ; X= Br **3a:** 73%y; 75:25er
XI R^1= H; R^2= 4-CF_3-Ph ; X= Br **3a:** 97%y; 76:24er
XII R^1= H; R^2= 4-*t*-Bu-Ph ; X= Br **3a:** 63%y; 68:32er
XIII R^1= H; R^2= 2-CF_3-Ph ; X= Br **3a:** 47%y; 57:43er
XIV R^1= H; R^2= 2-NO-Ph ; X= Br **3a:** 57%y; 55:45er
XV R^1= H; R^2= 2-OMe-Ph ; X= Br **3a:** 94%y; 63:37er
XVI R^1= H; R^2= 2-CN-Ph ; X= Br **3a:** 69%y; 56:44er
XVII R^1= H; R^2= 2,3-$(F)_2$-Ph ; X= Br **3a:** 59%y; 70:30er
XVIII R^1= H; R^2= 3,4,5-$(F)_3$-Ph ; X= Br **3a:** 63%y; 78:22er
XIX R^1= H; R^2= 2,3,4,5,6-$(F)_5$-Ph; X= Br **3a:** 80%y; 72:28er
XX R^1= H; R^2= 2,3,5,6-$(F)_4$-4-CF_3-Ph ; X= Br **3a:** 80%y; 73:27er
XXI R^1= H; R^2= 9-anthracenyl ; X= Br **3a:** 27%y; 76:24er

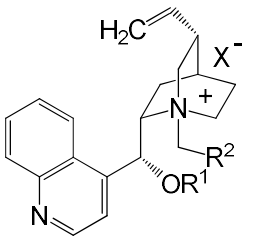

XXII R^1=H; R^2= Ph; X= Cl **3a:** 70%y; 58:42er
XXIII R^1=Ph; R^2= Ph; X= Br **3a:** 72%y; 50:50er
XXIV R^1=Ph; R^2= 2,3,4-$(F)_3$-Ph; X= Br **3a:** 88%y; 55:45er
XXV R^1=H; R^2= 9-anthracenyl; X= Cl **3a:** 69%y; 65:35er

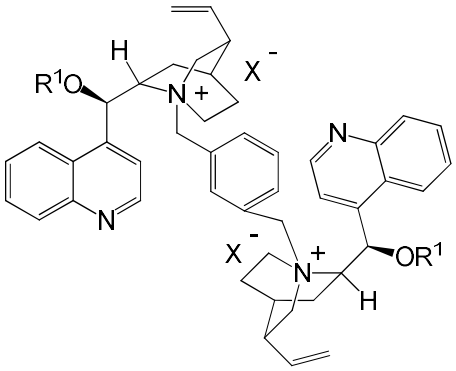

XXVI R^1= H; X= Br **3a:** 46%y; 62:38er
XXVII R^1= Bn; X= Br **3a:** 85%y; 60:40er

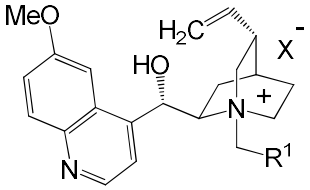

VIII R^1= 3,5-$(CF_3)_2$-Ph; X= Br **3a:** 49%y; 82:18er
XXVIII R^1= 4-NO_2-Ph; X= Br **3a:** 44%y; 78:22er
XXIX R^1= 2,3,4-$(F)_3$-Ph; X= Br **3a:** 46%y; 70:30er
XXX R^1= 3,4,5-$(F)_3$-Ph; X= Br **3a:** 34%y; 80:20er

Screening of reaction conditions for asymmetric trifluoromethylthiolation of 1e

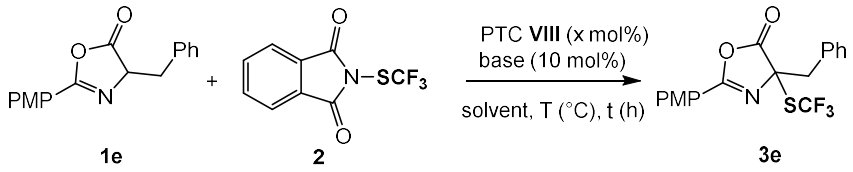

entry	Base	solvent	(x mol%)	T (°C)	t (h)	yield (%)[a]	er[b]
1	K_3PO_4	DCM	20	-20	1	84	94:6
2[c]	K_3PO_4	DCM	20	-20	4	89	75:25
3	K_2CO_3	DCM	20	-20	1	80	83:17
4	Cs_2CO_3	DCM	20	-20	1	79	86:14
5	$NaHCO_3$	DCM	20	-20	1	83	88:12
6	KF	DCM	20	-20	1	82	90:10
7	K-Phthalimide	DCM	20	-20	2	83	80:20
8	K_3PO_4	$CHCl_3$	20	-20	6	83	83:17
9	K_3PO_4	Et_2O	20	-20	2	87	76:24
10	K_3PO_4	THF	20	-20	1	85	67:33
11	K_3PO_4	DCE	20	-20	3	88	72:28
12	K_3PO_4	toluene	20	-20	6	88	83:17
13	K_3PO_4	DCM	10	-20	1	86	90:10
14	K_3PO_4	DCM	5	-20	1	87	89:11
15	K_3PO_4	DCM	2	-20	1	89	86:14
16	K_3PO_4	DCM	20	-40	3	82	91:9
17	K_3PO_4	DCM	20	-70	6	85	87:13

[a] Isolated yield. [b] Determined by HPLC on a chiral stationary phase. [c] Reaction performed with 5 mol% of K_3PO_4.

Trifluoromethylthiolation of azlactones 1a-e promoted by TBAB

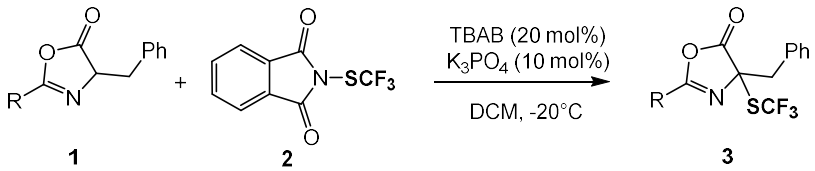

1 2 3

entry	R	t (h)	yield (%)[a]
1	4-CN(C_6H_4)	168	Degradation
2	4-CF_3(C_6H_4)	168	Degradation
3	C_6H_5	96	47
4	4-Cl(C_6H_4)	19	60
5	4-OMe(C_6H_4)	1	80

[a] Isolated yield.

Experimental and theoretical circular dichroism spectra of compound 3k

Electronic Circular Dichroism (CD) spectra were experimentally obtained at 25°C on a Jasco-815 CDspectrometer including a Jasco Peltier ETCT-762 temperature controller. Measurements were performed using quartz cuvettes (1cm), (c = 5.2E-5 in DCM spectroscopic grade). The CD spectra were also simulated by means of density functional (DFT) simulations. To this we optimized the geometry of compound 3k at the CAM-B3LYP/cc-pVTZ level of theory, i.e. with the long-range-corrected version of B3LYP using the attenuating method[7]. Solvent effects (dichloromethane) were included within the Polarizable Continuum Model (PCM) using the integral equation formalism variant (IEFPCM)[8]. The same method was used to compute the CD spectra[9] within the time-dependent density functional theory (TDDFT)[10]. Figure S1 represents the experimental CD spectra of **3k** and the simulated one for both enantiomers, allowing to disentangle the chirality easily with the first two bands (transitions observed between 300 and 250 nm).

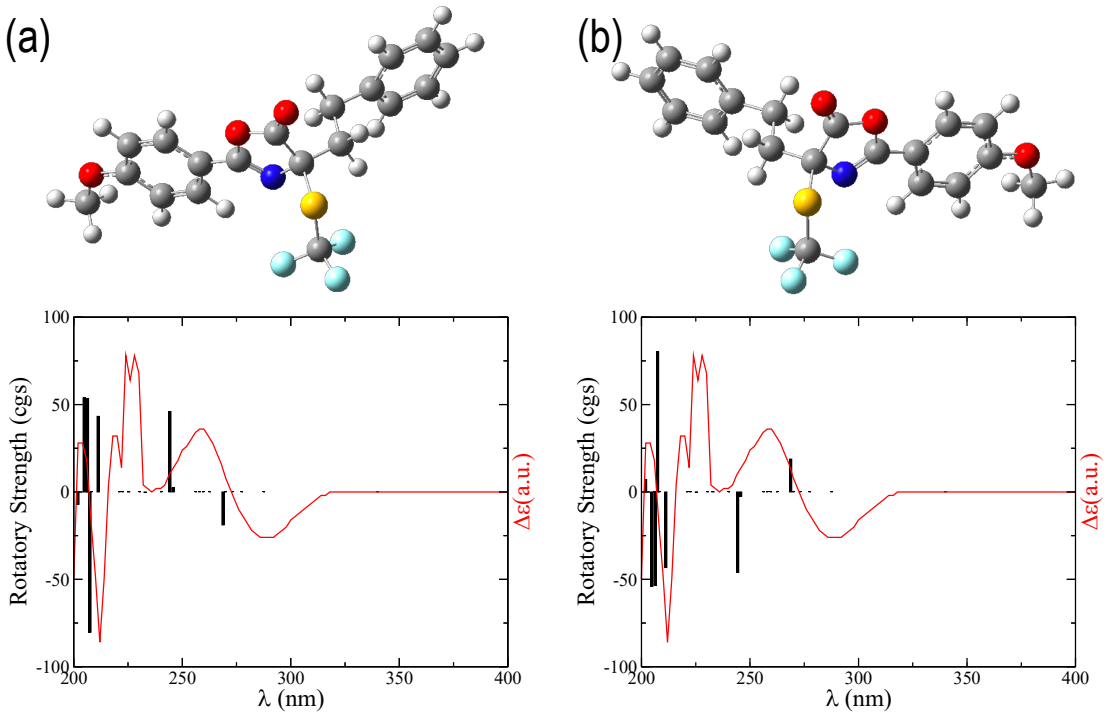

Figure S1. Experimentally measured CD spectra of compound **3k** (red curve) and simulation for both enantiomers (black bars). We can conclude that the measured spectra correspond to the left one, i.e. the **3k** *R* enantiomer.

DFT calculations

The density functional theory (DFT) calculations were performed using the M062x functional[11], specially developed to correctly reproduce non-covalent interactions, in combination with the 6-31++G(d,p) basis set, which includes both polarization and diffusion functions. Solvent effects (dichloromethane) were included within the Polarizable Continuum Model (PCM) using the integral equation formalism variant (IEFPCM)[8]. Atomic charges were computing within a Natural Bond Orbital analysis, using NBO version 3[12].

References

1. K. Kang, C. Xu and Q. Shen, *Org. Chem. Front.*, 2014, **1**, 294.

2. Y. Liu, B. A. Provencher, K. J. Bartelson and L. Deng, *Chem. Sci*., 2011, **2**, 1301.

3. S.-s. Jew, B.-S. Jeong, M.-S. Yoo, H. Huh and H.-g. Park, *Chem. Commun*., 2001, **14**, 1244.

4. C. Macovei, P. Vicennati, J. Quinton, M. C. Nevers, H. Volland, C. Creminon and F. Taran, *Chem. Commun.,* 2012, **48**, 4411.

5. A. D. Melhado, M. Luparia and F. D. Toste, *J. Am. Chem. Soc*., 2007, **129**, 12638.

6. a) S. K. Nimmagadda, M. Liu, M. K. Karunananda, D.-W. Gao, Omar Apolinar, J. S. Chen, P. Liu and K. M. Engle, *Angew. Chem. Int. Ed*., 2019, **58**, 3923; b) Y. Wang, Y. Chen, X. Li, Y. Mao, W. Chen, R. Zhan and H. Huang, *Org. Biomol. Chem*., 2019, **17**, 3945; c) D. Uraguchi, Y. Ueki, A. Sugiyama and T. Ooi, *Chem. Sci*., 2013, **4**, 1308; d) H. Hu, Y. Liu, J. Guo, L. Lin, Y. Xu, X. Liua and X. Feng, *Chem. Commun*., 2015, **51**, 3835; e) T. Takafumi, T. Tsukushi, T. Taro, Y. Ryo and O. Takashi, *Org. Lett*., 2018, **21**, 3541; f) T. Wang, Z. Yu, D. L. Hoon, C. Y. Phee, Y. Lan and Y. Lu, *J. Am. Chem. Soc*., 2016, **138**, 265.

7. T. Yanai, D. Tew, and N. Handy, *Chem. Phys. Lett.*, 2004, **393**, 51.

8. J. Tomasi, B. Mennucci, and R. Cammi, *Chem. Rev.*, 2005, **105**, 2999.

9. J. Autschbach, T. Ziegler, S.J.A. van Gisbergen, and E.J. Baerends, *J. Chem. Phys.*, 2002, **116**, 6930.

10. M.E. Casida, C. Jamorski, K.C. Casida, and D.R. Salahub, *J. Chem. Phys.*, 1988, **108**, 4439.

11. Y. Zhao and D. G. Truhlar, *Theor. Chem. Acc.*, 2008, **120**, 215.

12. A. E. Reed, L. A. Curtiss, and F. Weinhold, *Chem. Rev.*, 1988, **88**, 899.

NMR Spectra

2-(4-methoxyphenyl)-4-(naphthalen-2-ylmethyl)oxazol-5(4*H*)-one (1f)

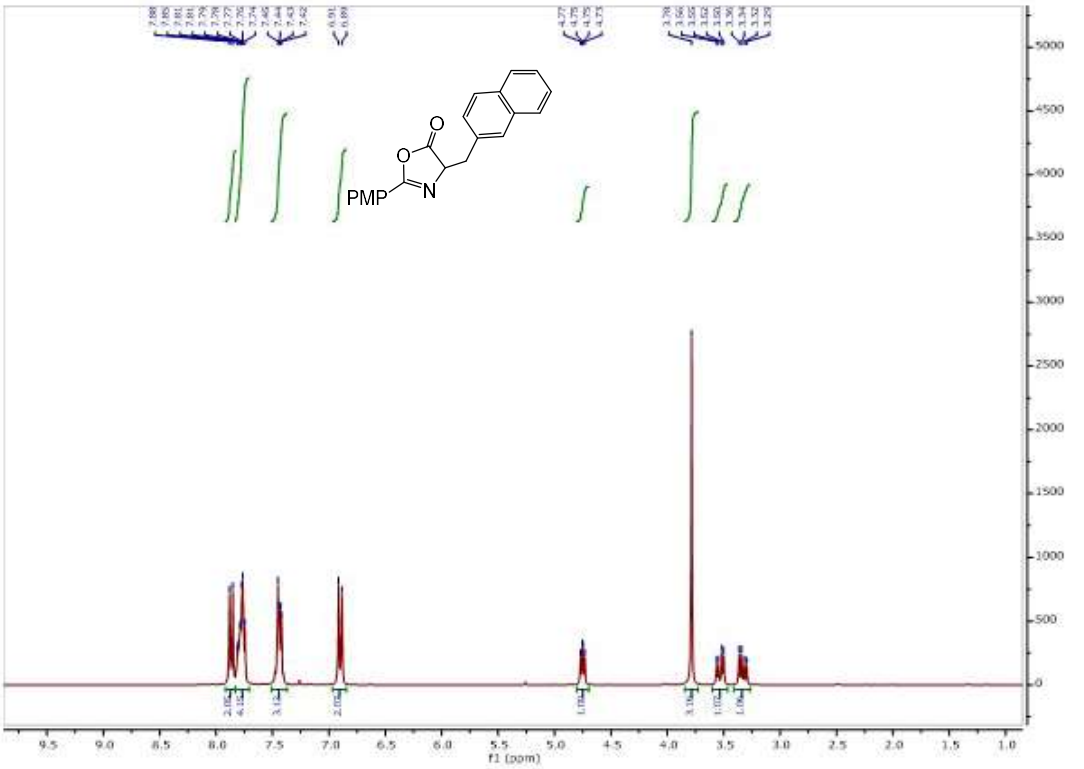

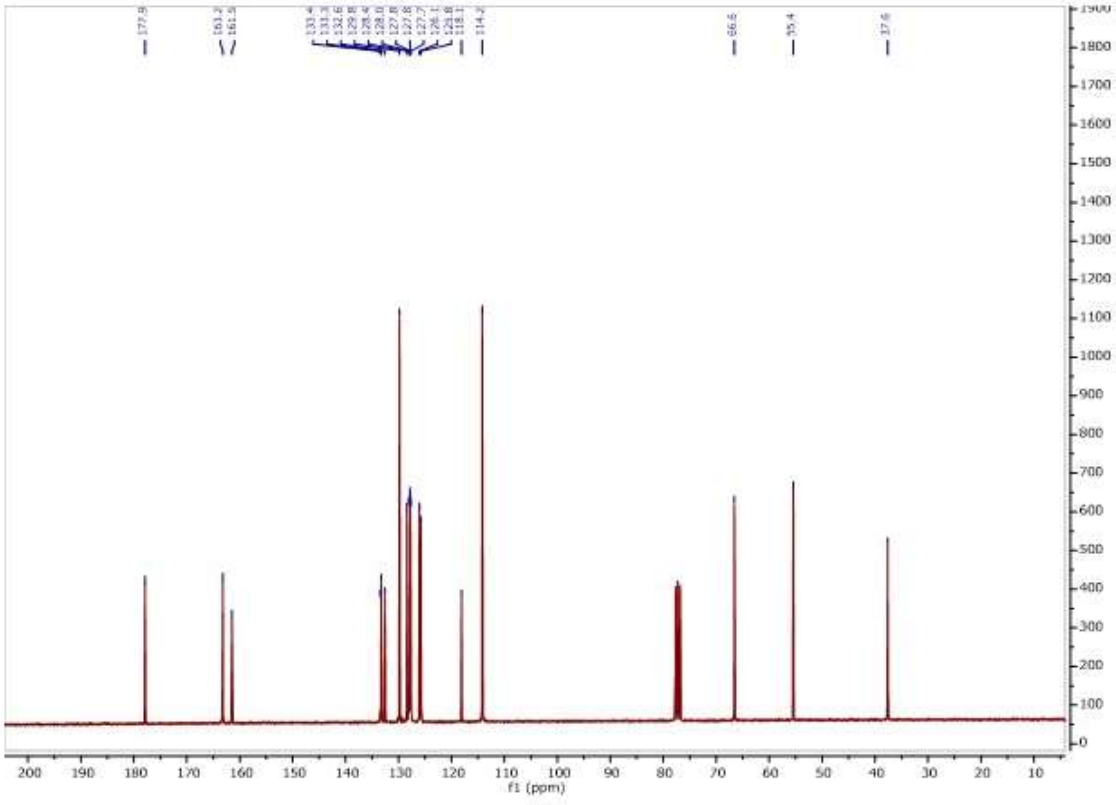

4-(3,4-dichlorobenzyl)-2-(4-methoxyphenyl)oxazol-5(4*H*)-one (1i)

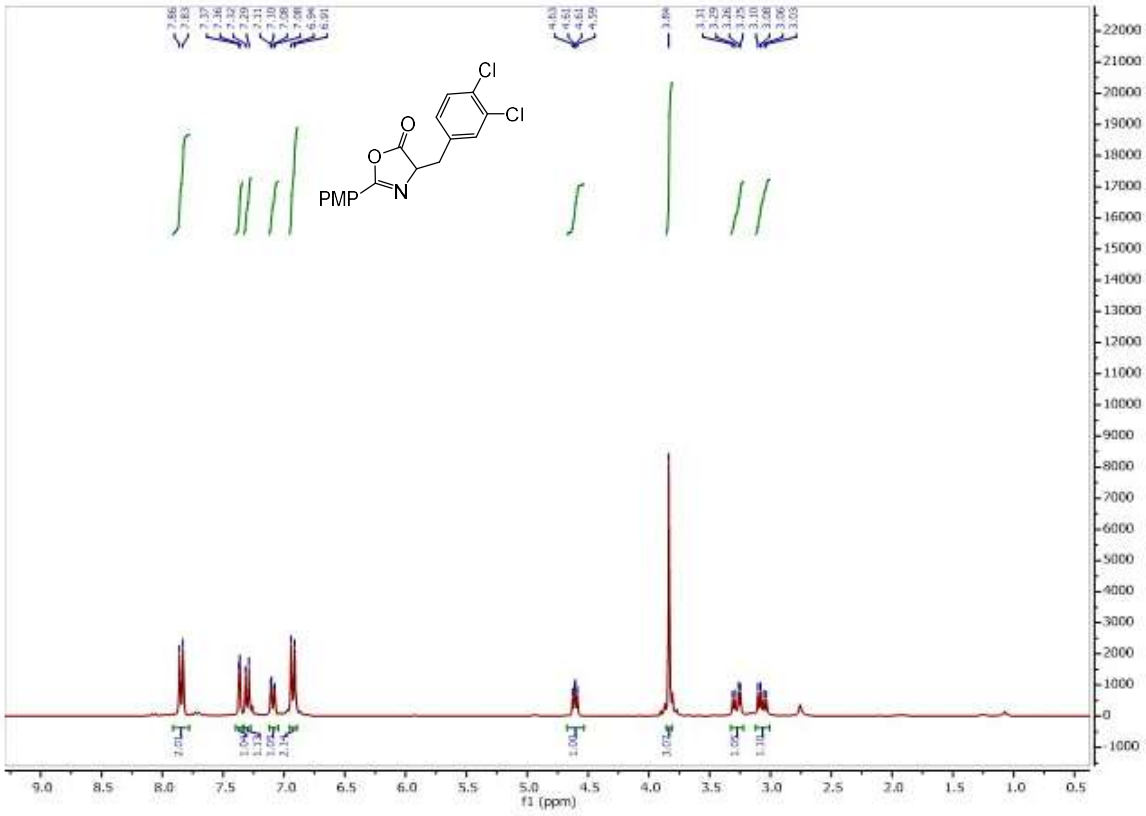

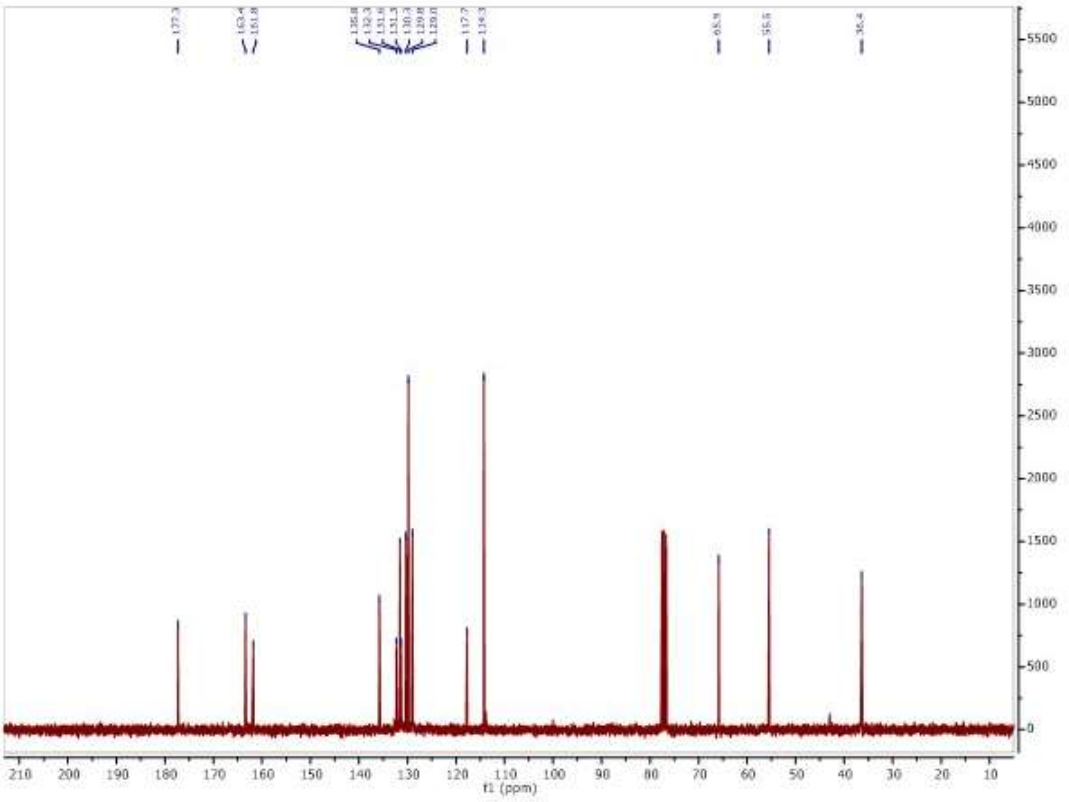

4-(cyclohexylmethyl)-2-(4-methoxyphenyl)oxazol-5(4*H*)-one (1m)

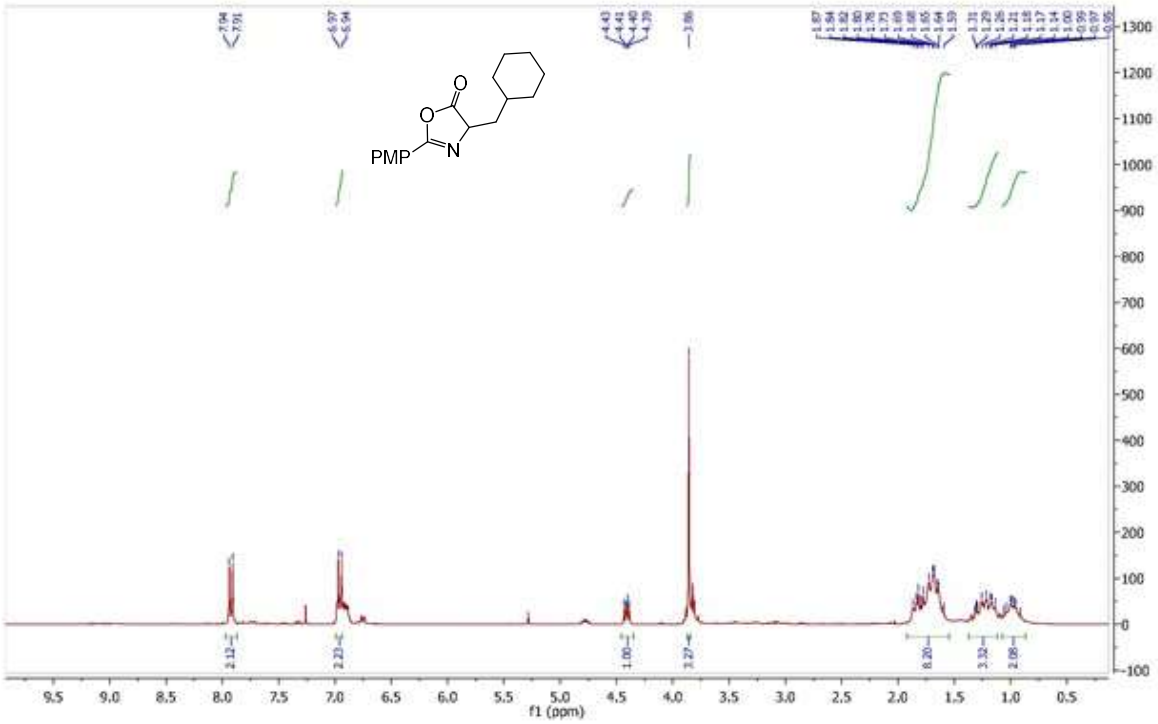

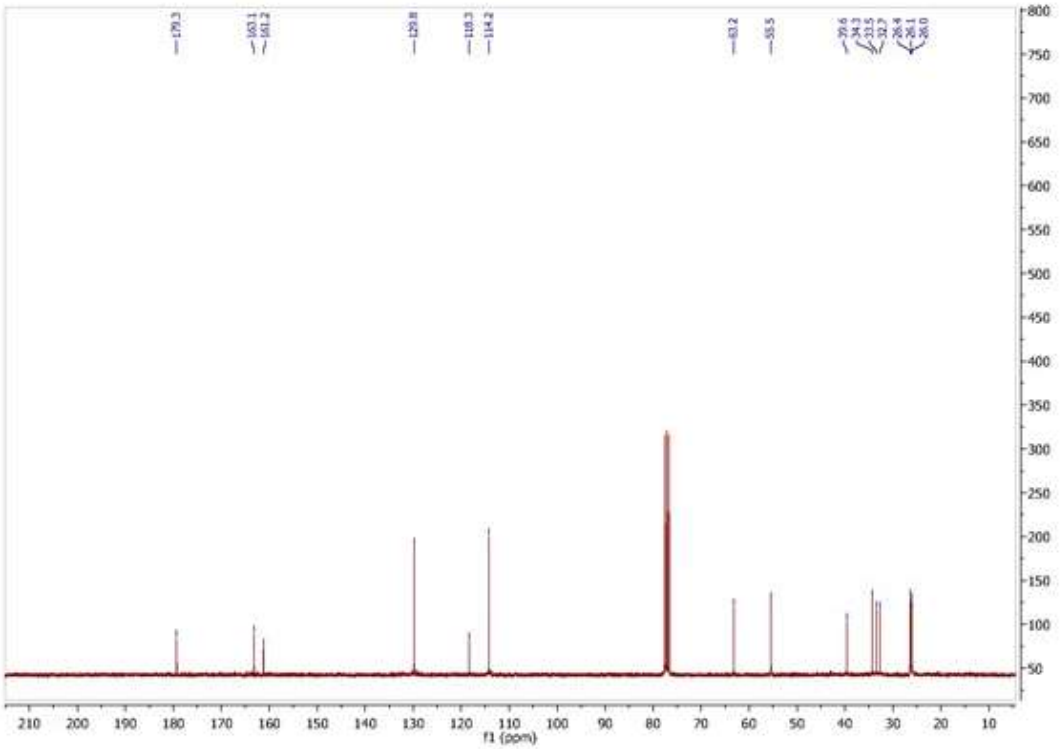

4-benzyl-2-(4-methoxyphenyl)-4-(trifluoromethyl)thio)oxazol-5(4*H*)-one (3e)

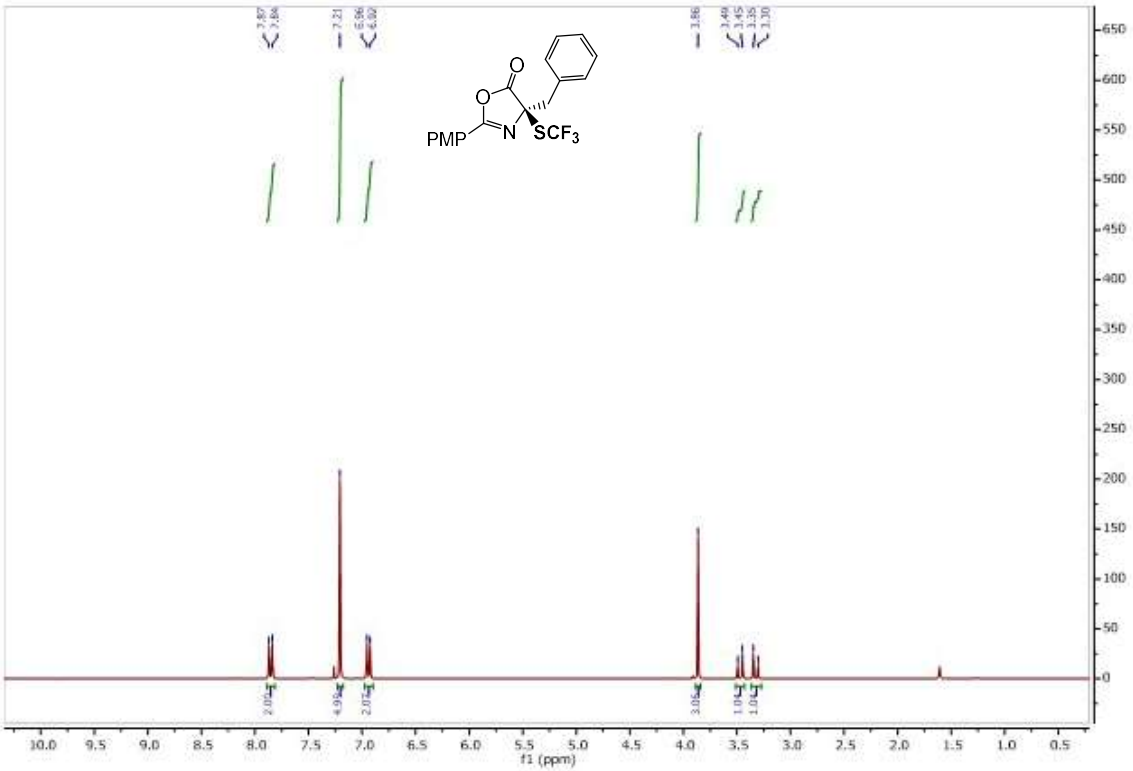

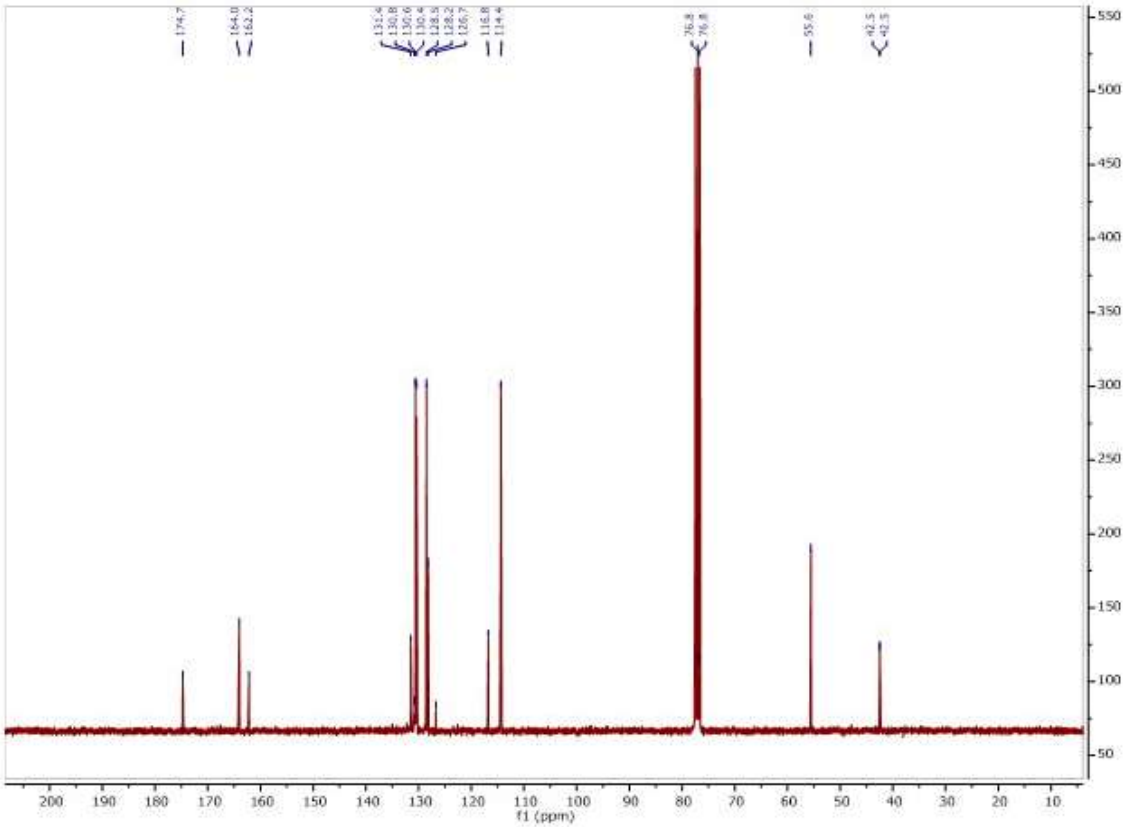

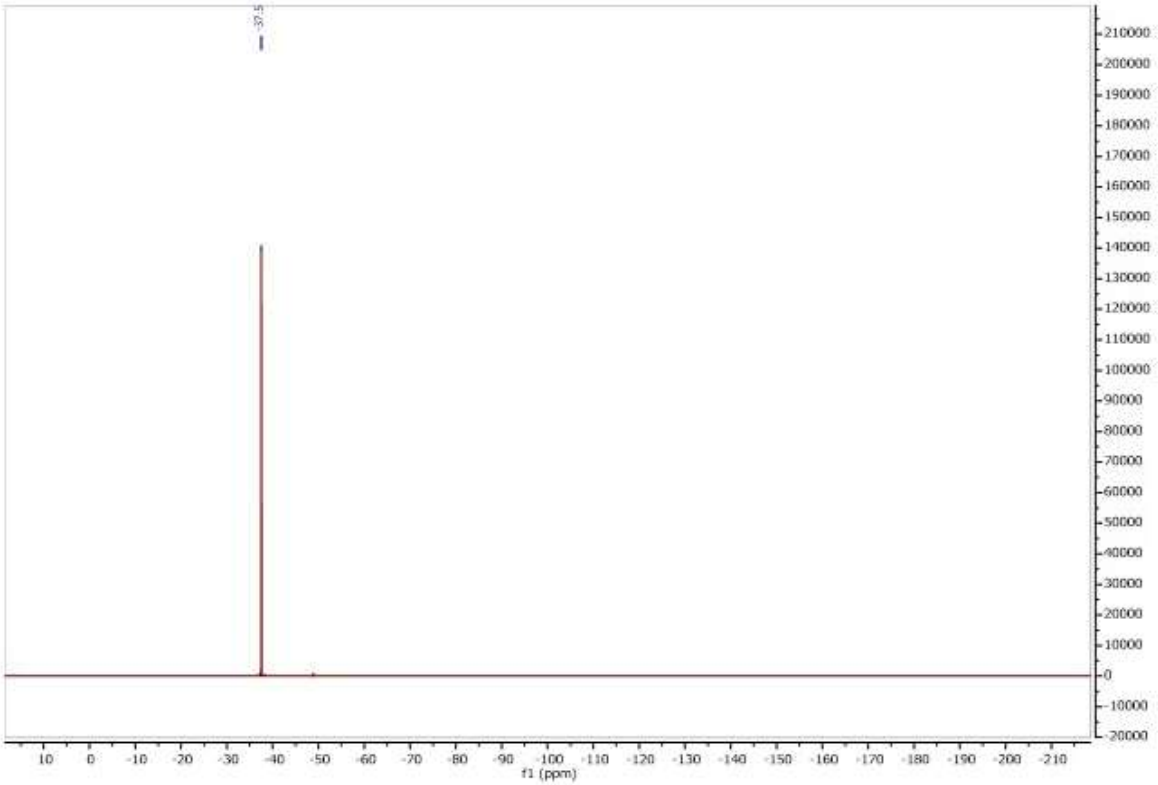

2-(4-methoxyphenyl)-4-(naphthalen-2-ylmethyl)-4-((trifluoromethyl)-thio)oxazol-5(4*H*)-one (3f)

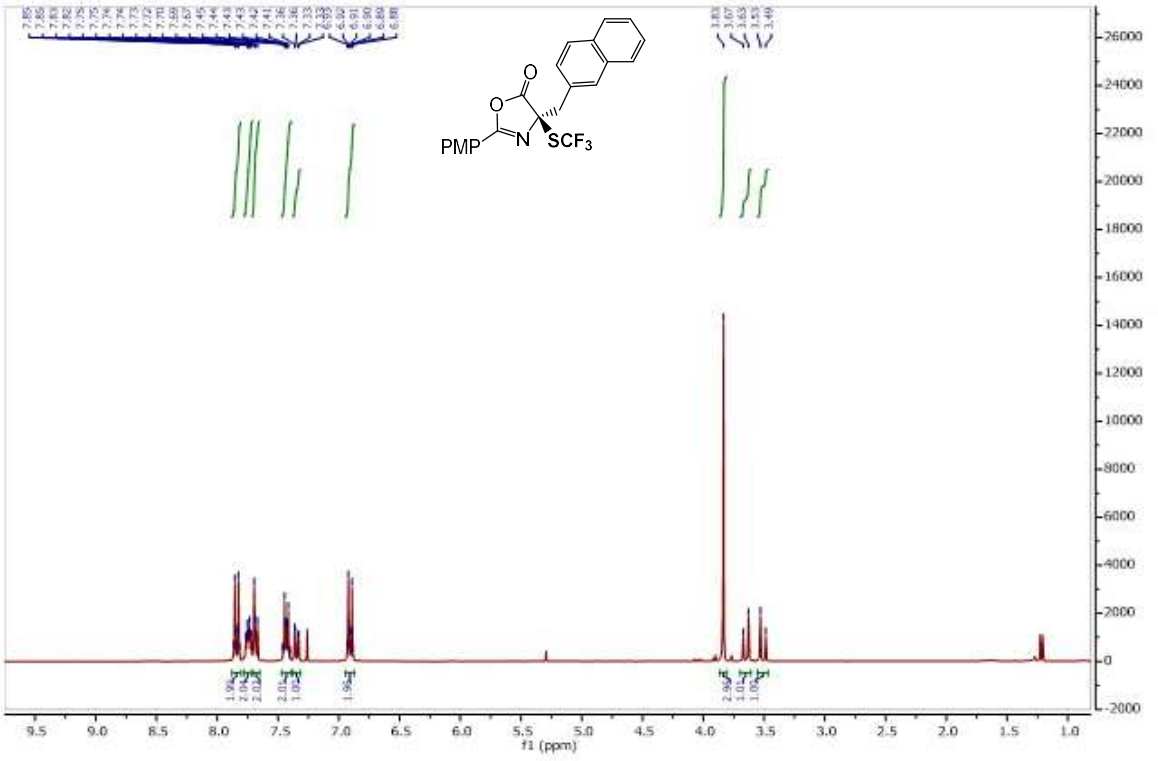

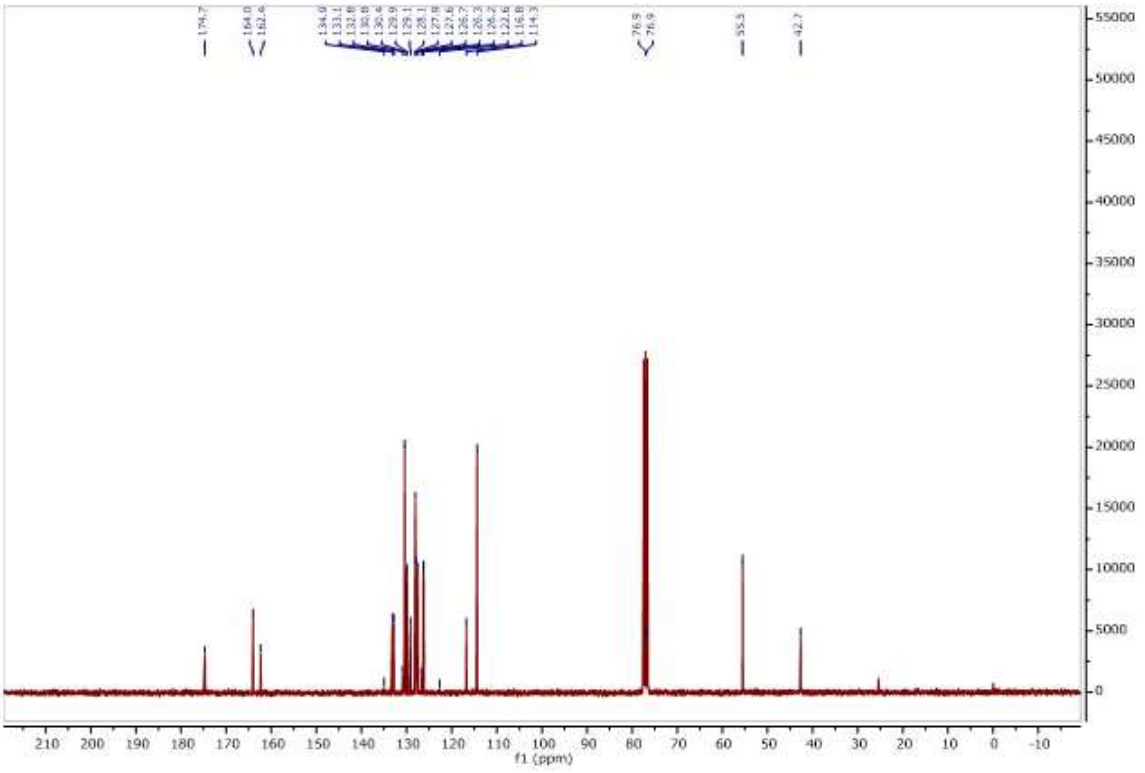
174.7
164.0
162.6
134.9
133.1
132.8
130.8
130.4
129.9
129.1
128.1
127.9
127.6
126.7
126.3
126.2
122.6
116.8
114.3
76.9
76.9
55.3
42.7
f1 (ppm)

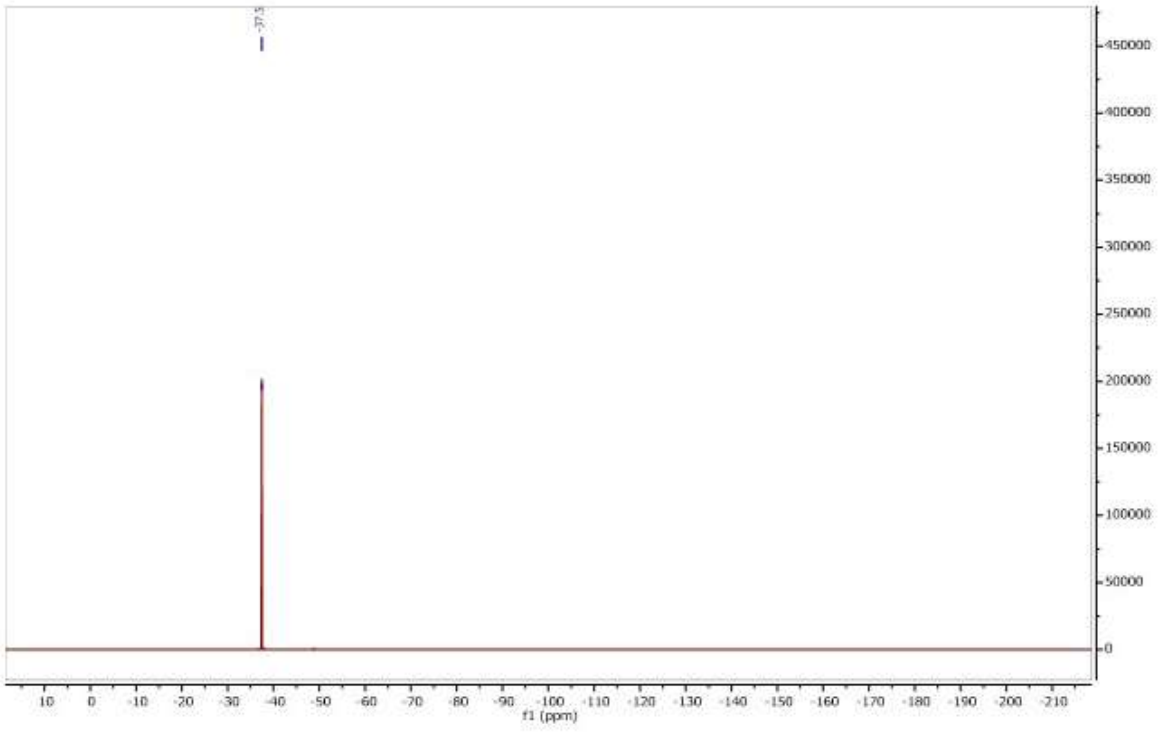
-37.5
f1 (ppm)

4-benzyl-2-(3,5-dimethoxyphenyl)-4-((trifluoromethyl)thio)oxazol-5(4*H*)-one (3g)

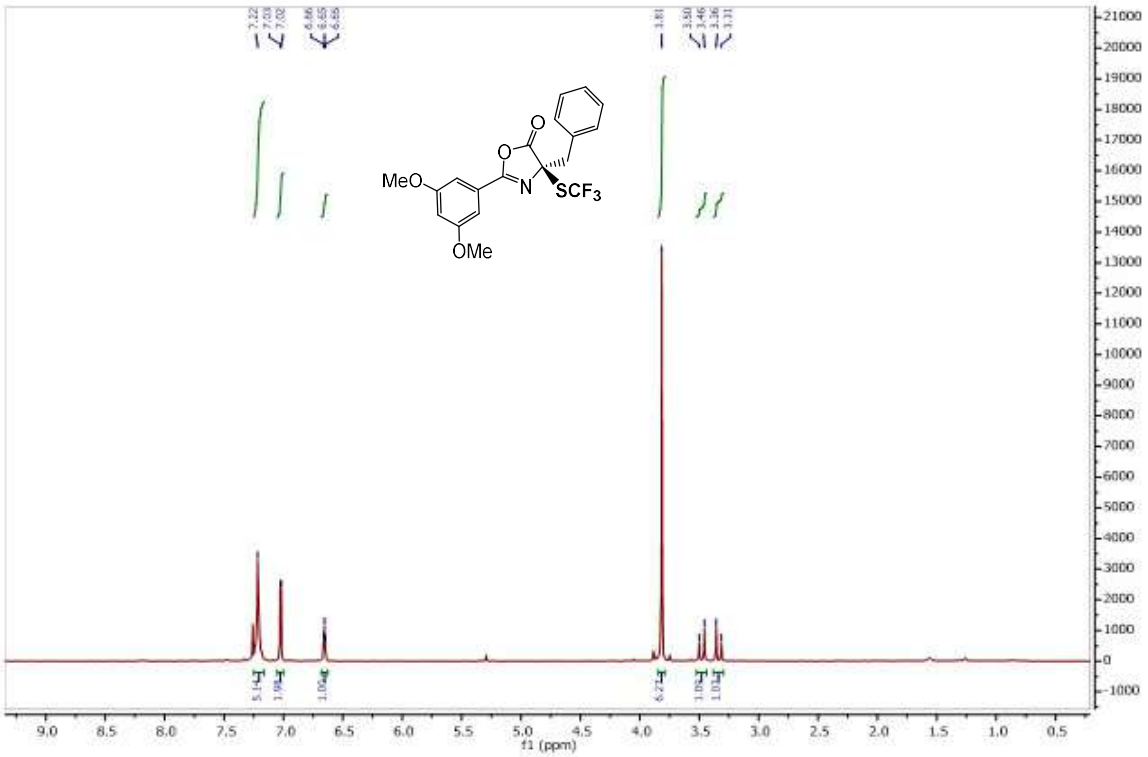

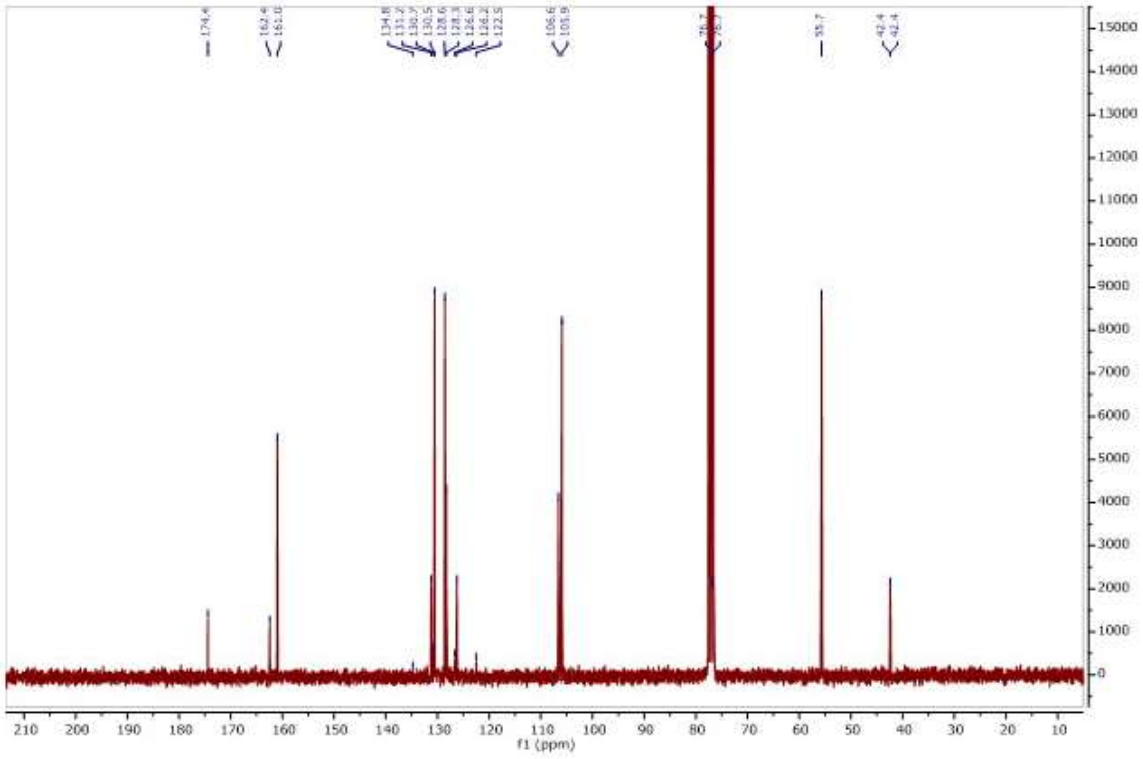

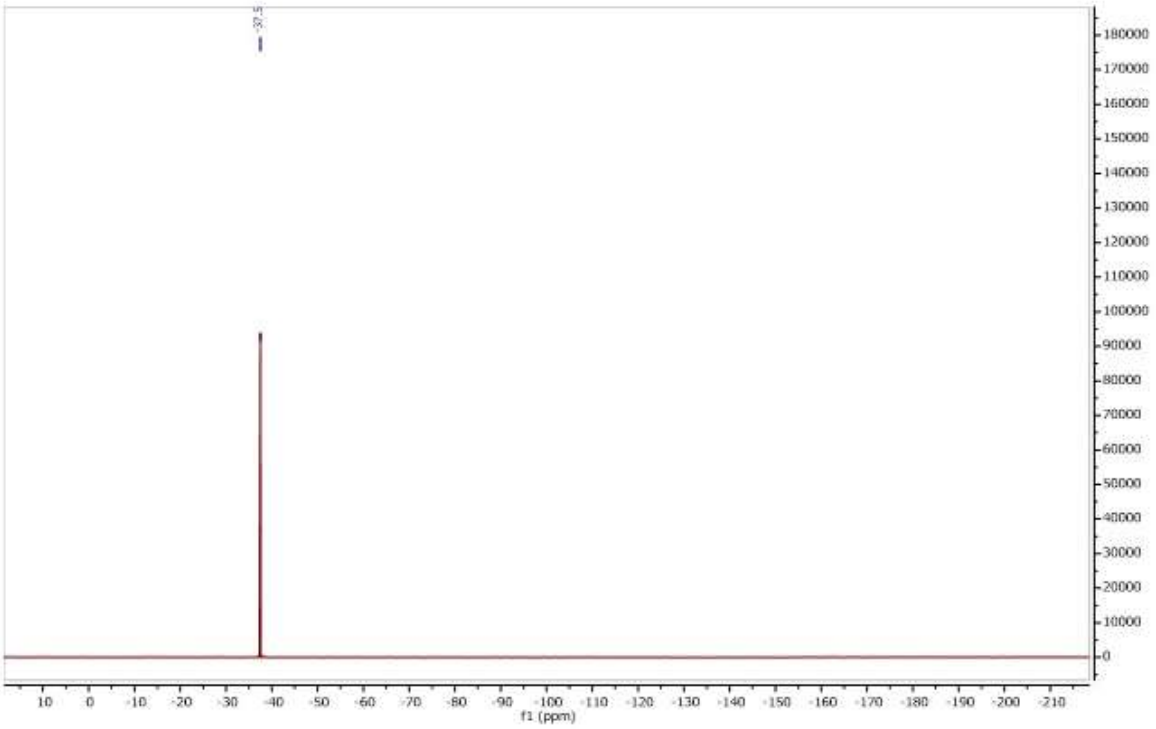

4-(3,4-dimethoxybenzyl)-2-(4-methoxyphenyl)-4-((trifluoromethyl)thio)oxazol-5(4*H*)-one (3h)

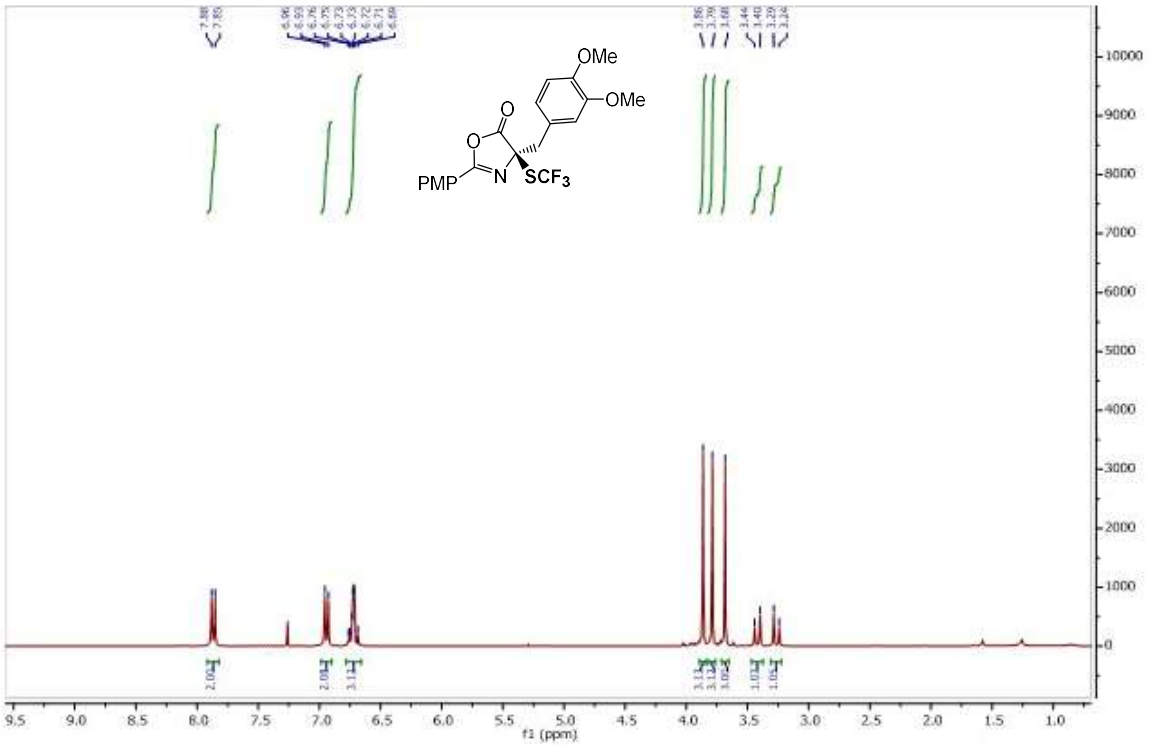

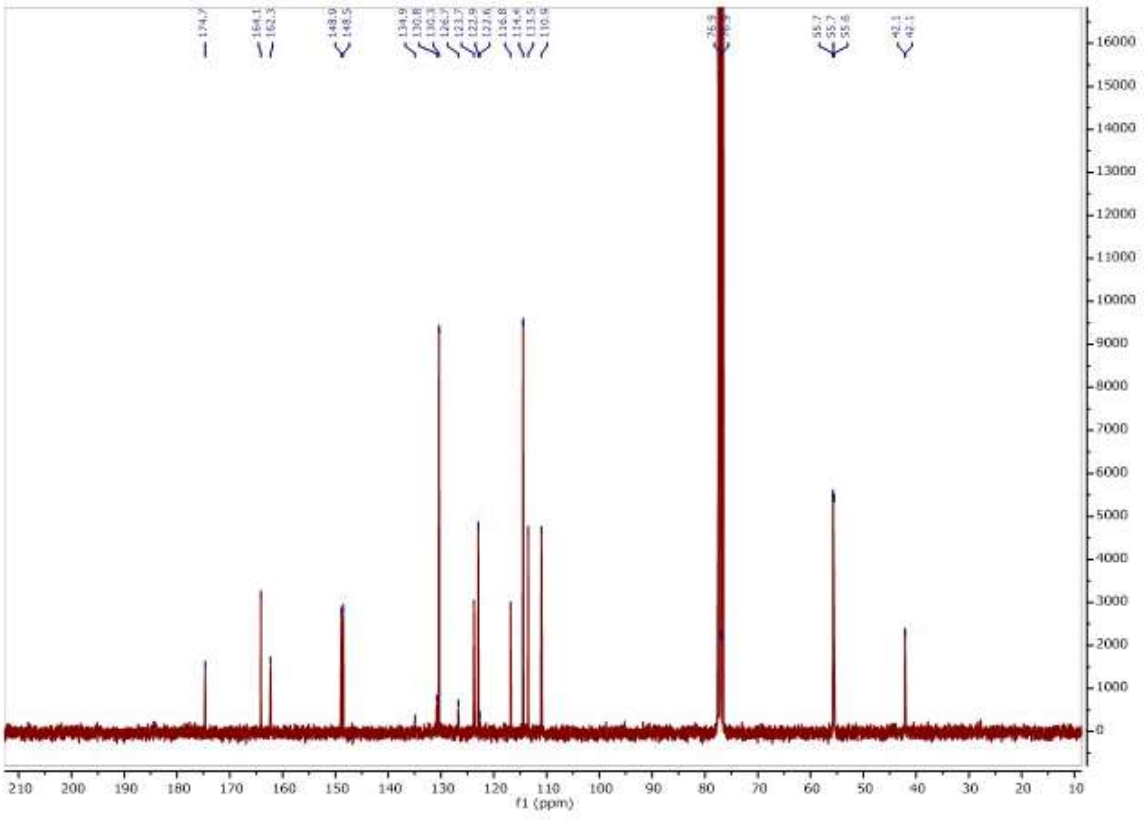
f1 (ppm)

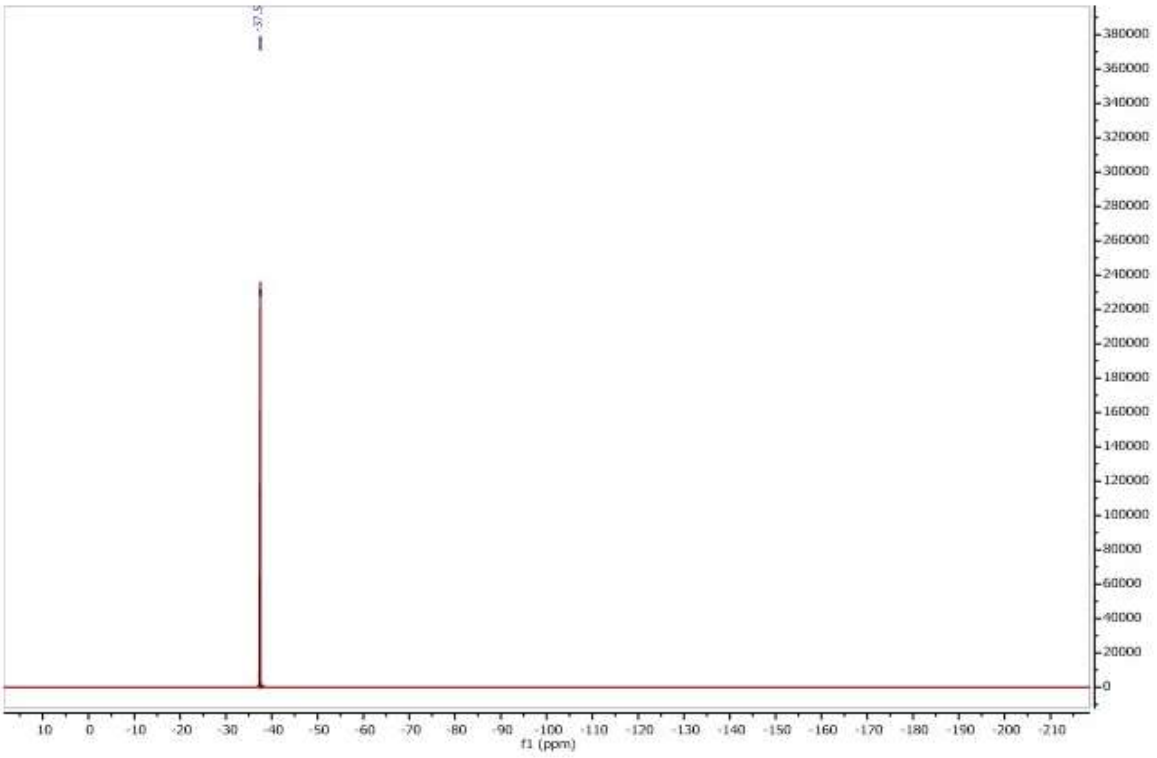
f1 (ppm)

4-(3,4-dichlorobenzyl)-2-(4-methoxyphenyl)-4-(trifluoromethyl)-thio)oxazol-5(4*H*)-one (3i)

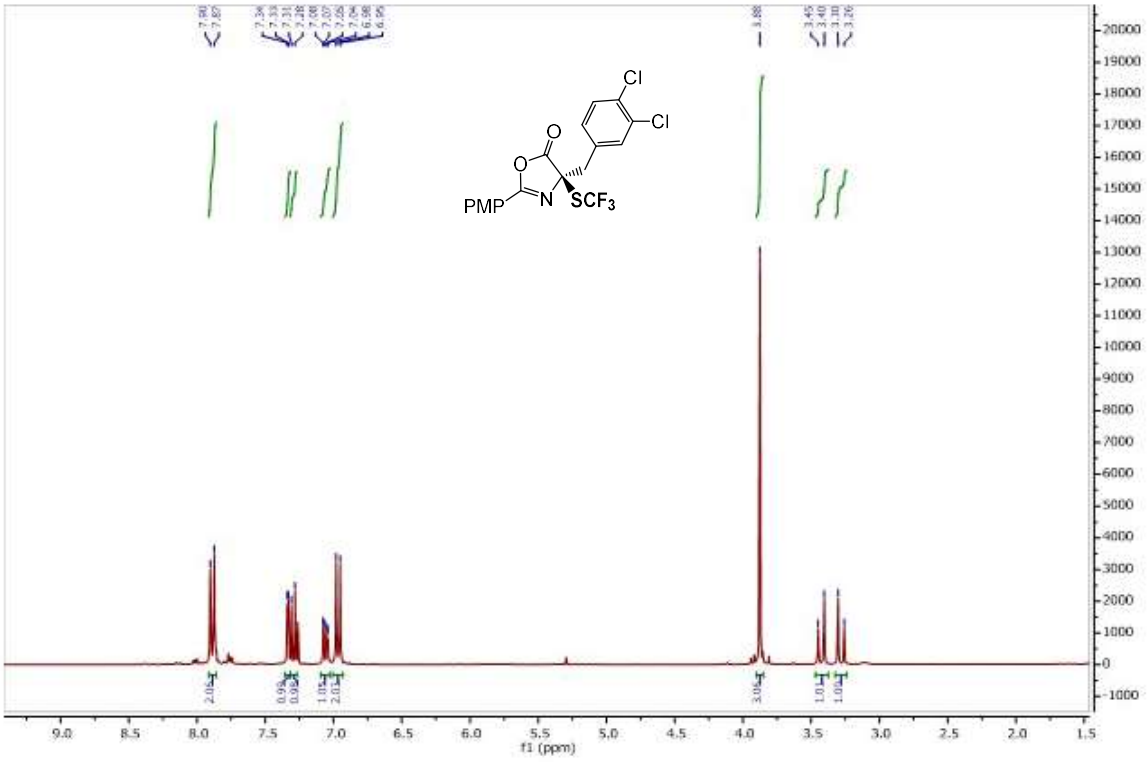

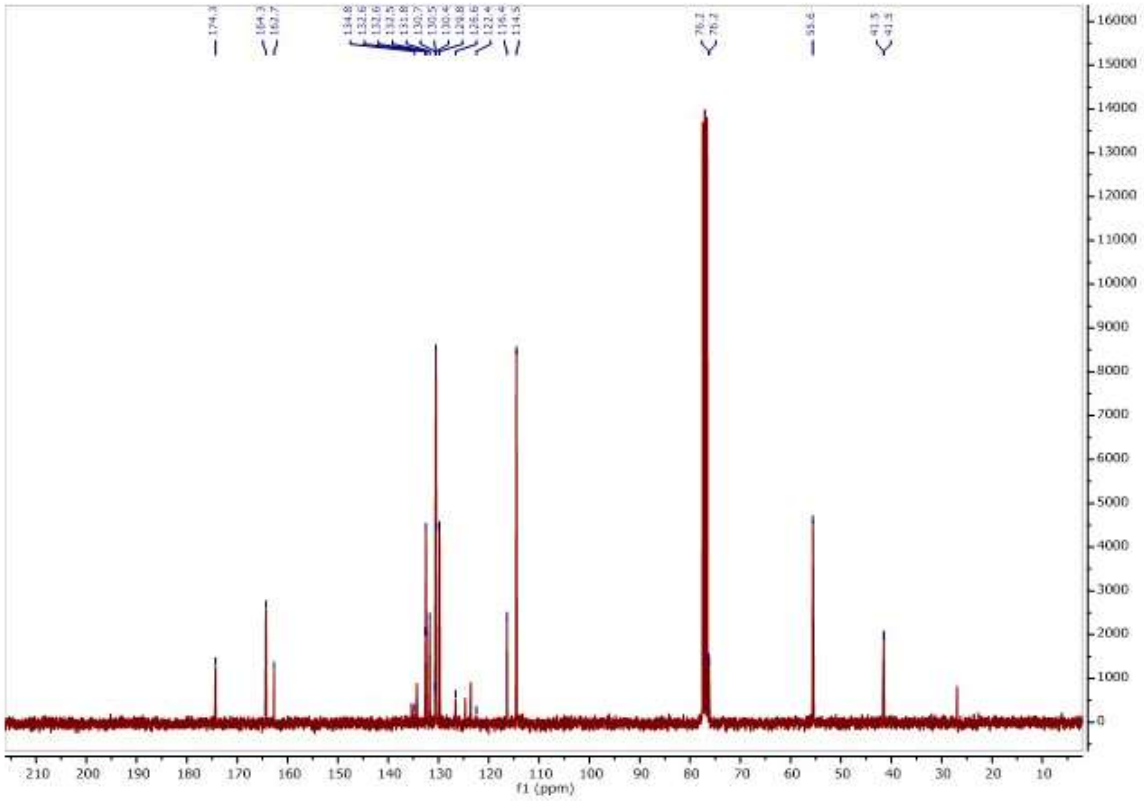

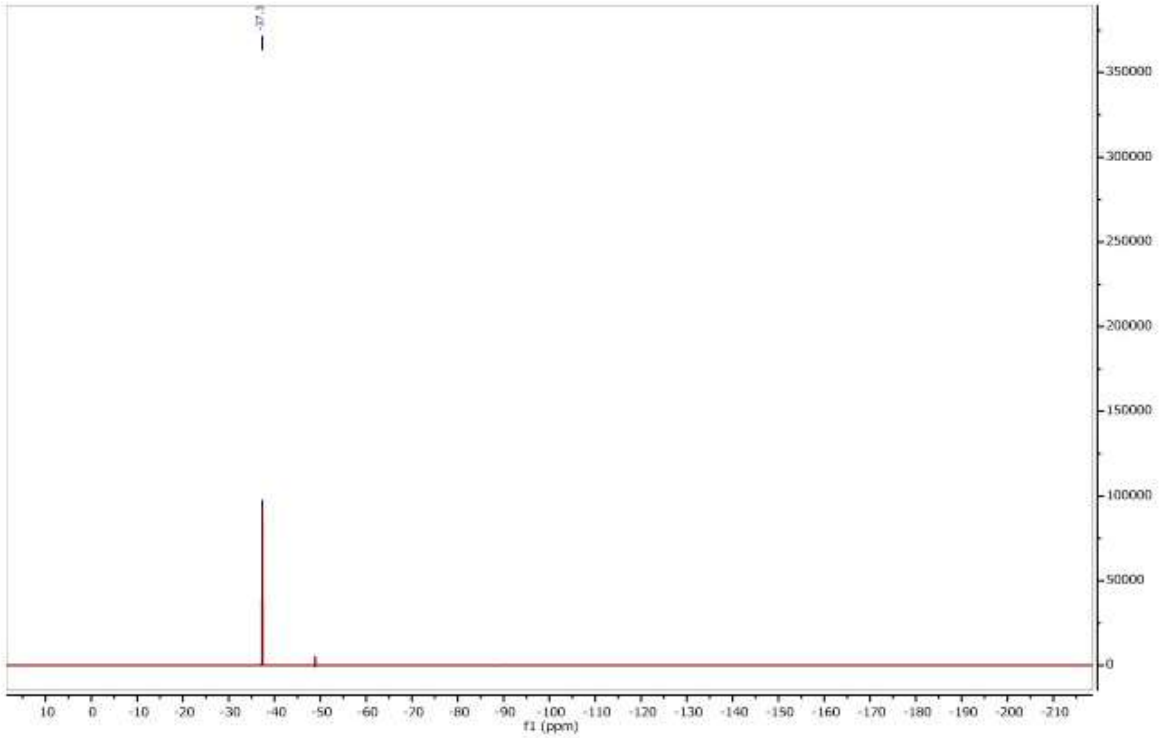

4-(4-chlorobenzyl)-2-(4-methoxyphenyl)-4-(trifluoromethyl)thio)oxazol-5(4*H*)-one (3j)

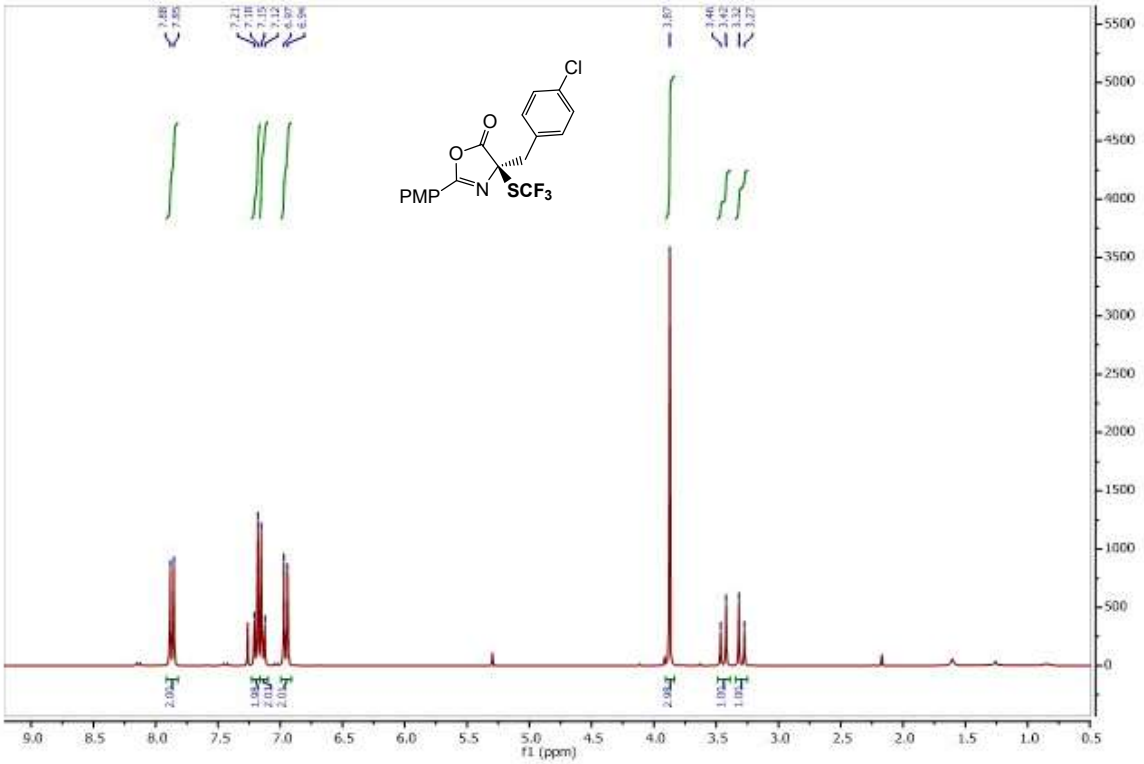

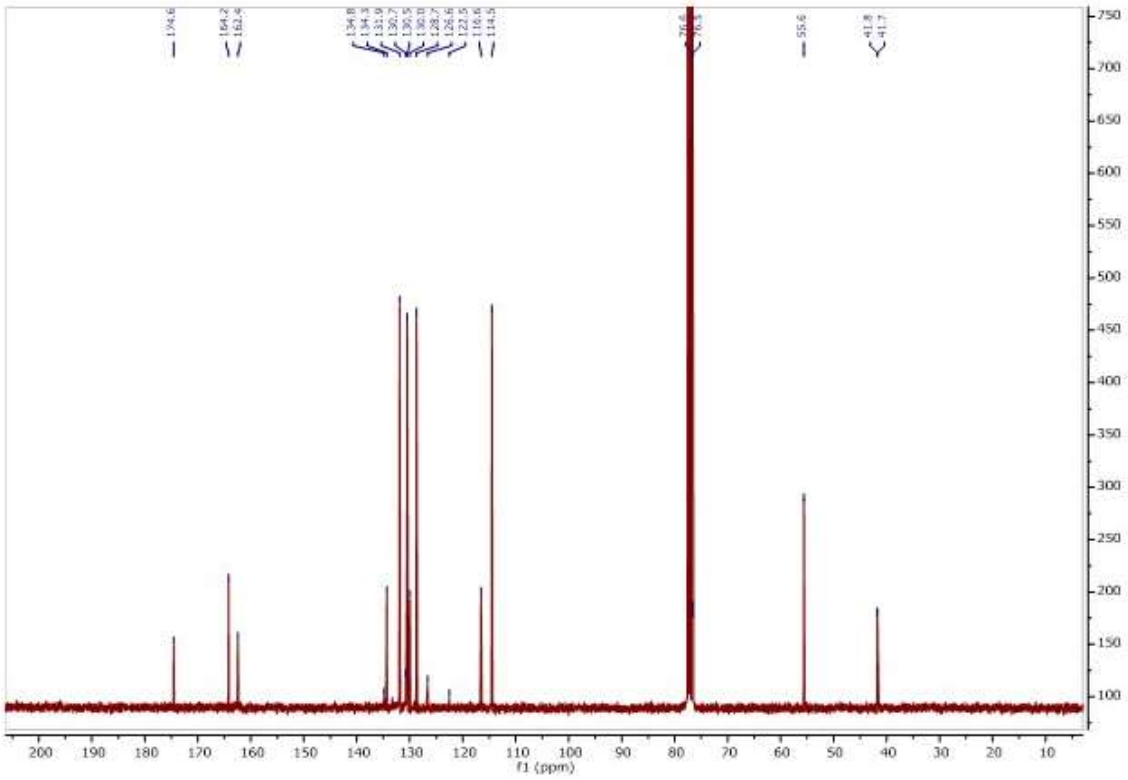
194.6
164.2
162.4
134.8
134.3
131.9
130.7
130.5
130.0
128.7
126.6
122.5
116.6
114.5
77.6
76.3
55.6
41.8
41.7
f1 (ppm)

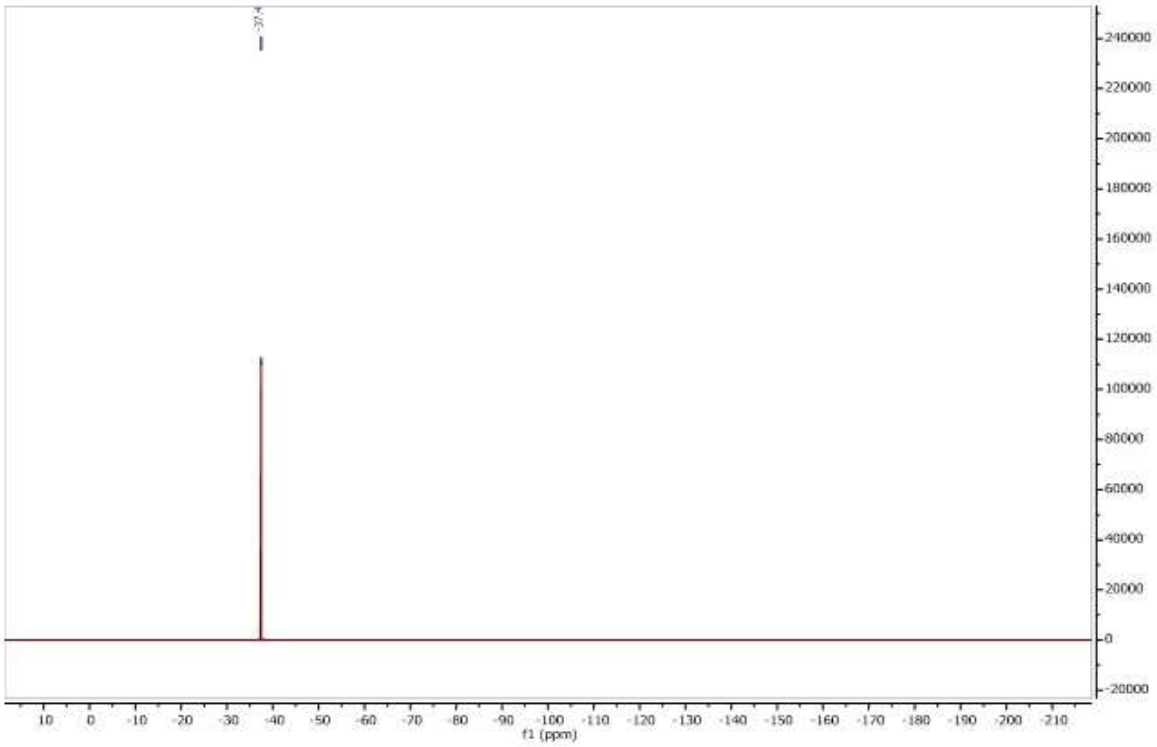
-37.4
f1 (ppm)

2-(4-methoxyphenyl)-4-phenethyl-4-((trifluoromethyl)thio)oxazol-5(4*H*)-one (3k)

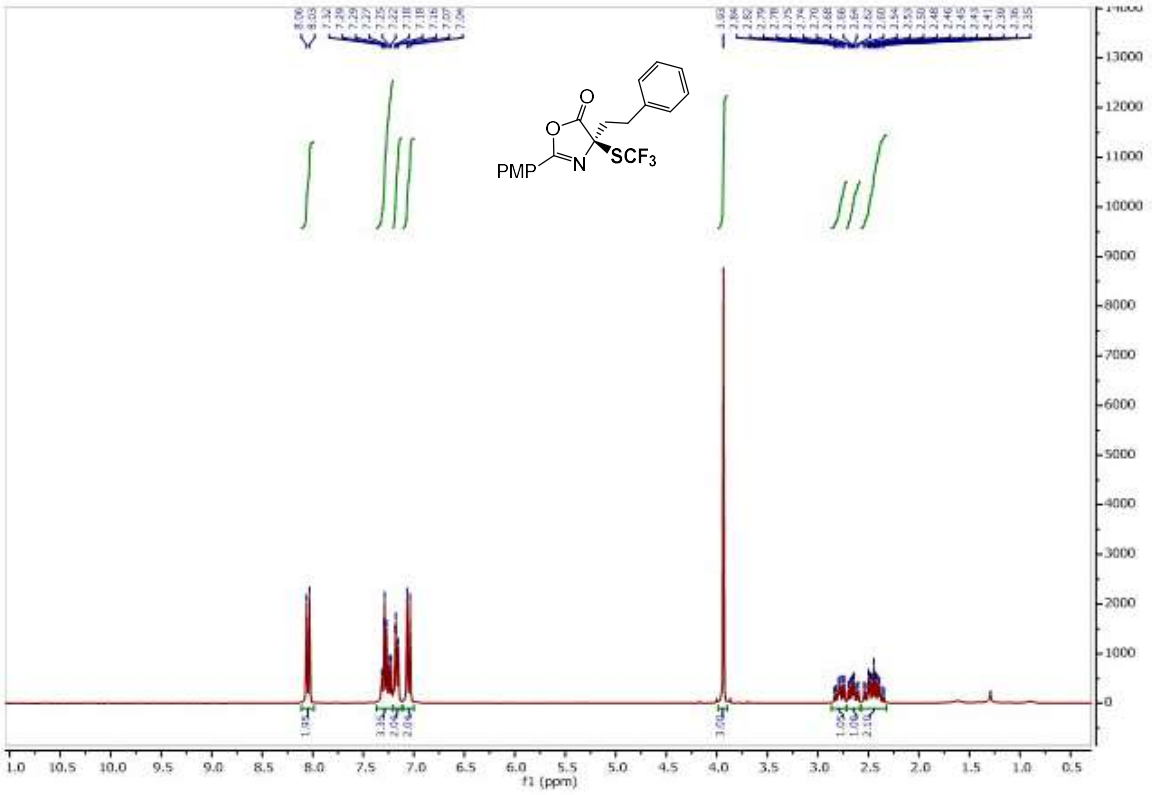

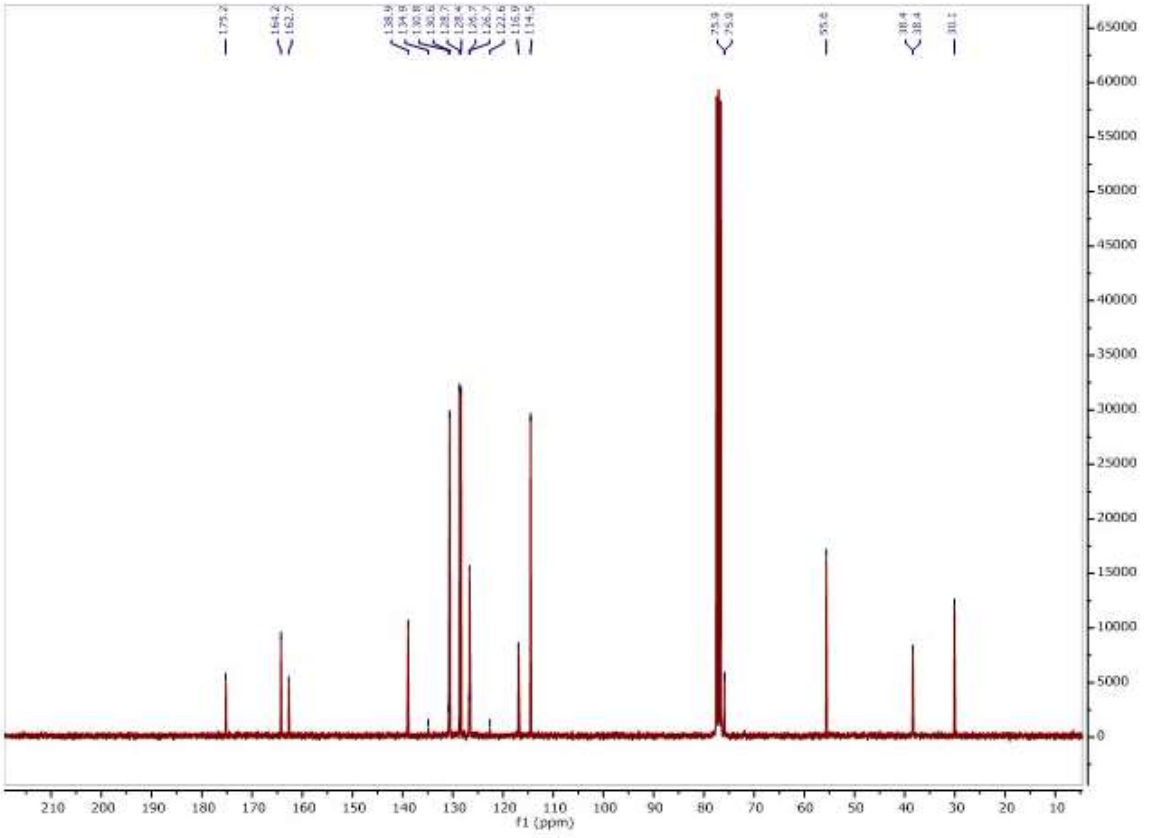

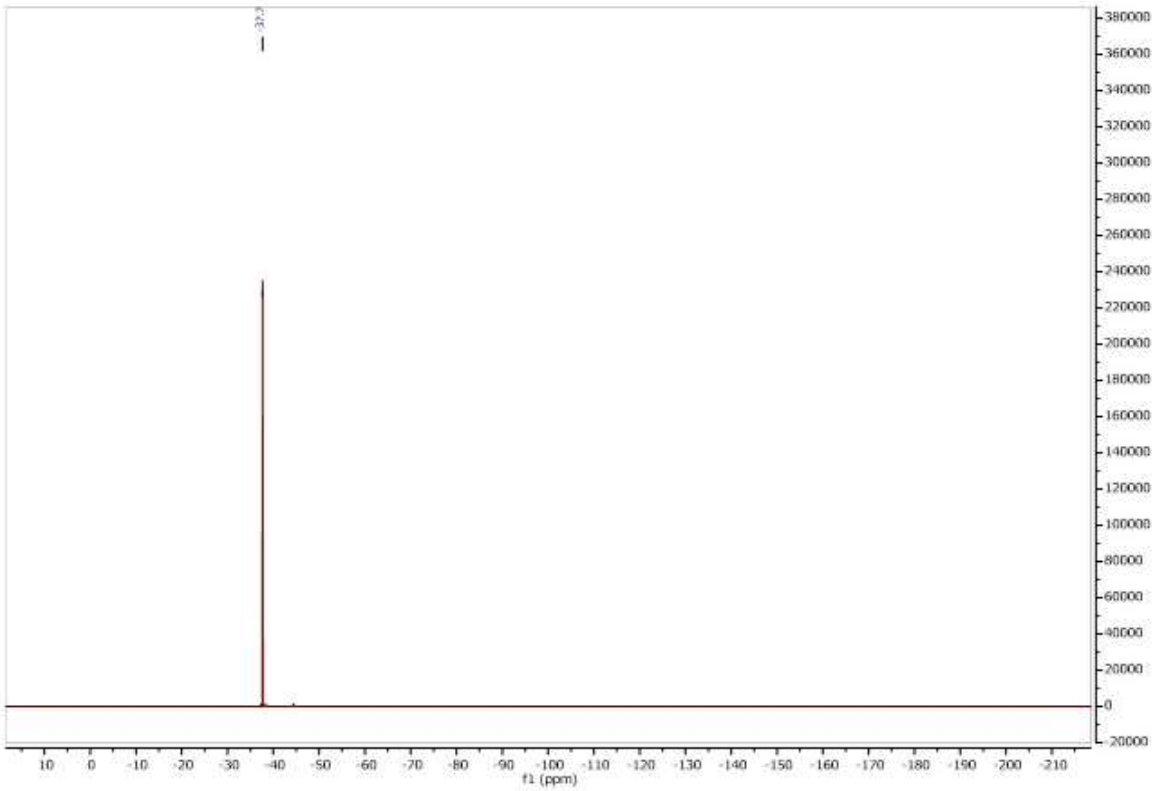

2-(4-methoxyphenyl)-4-(2-(ethylthio)ethyl)-4-((trifluoromethyl)thio)oxazol-5(4*H*)-one (3l)

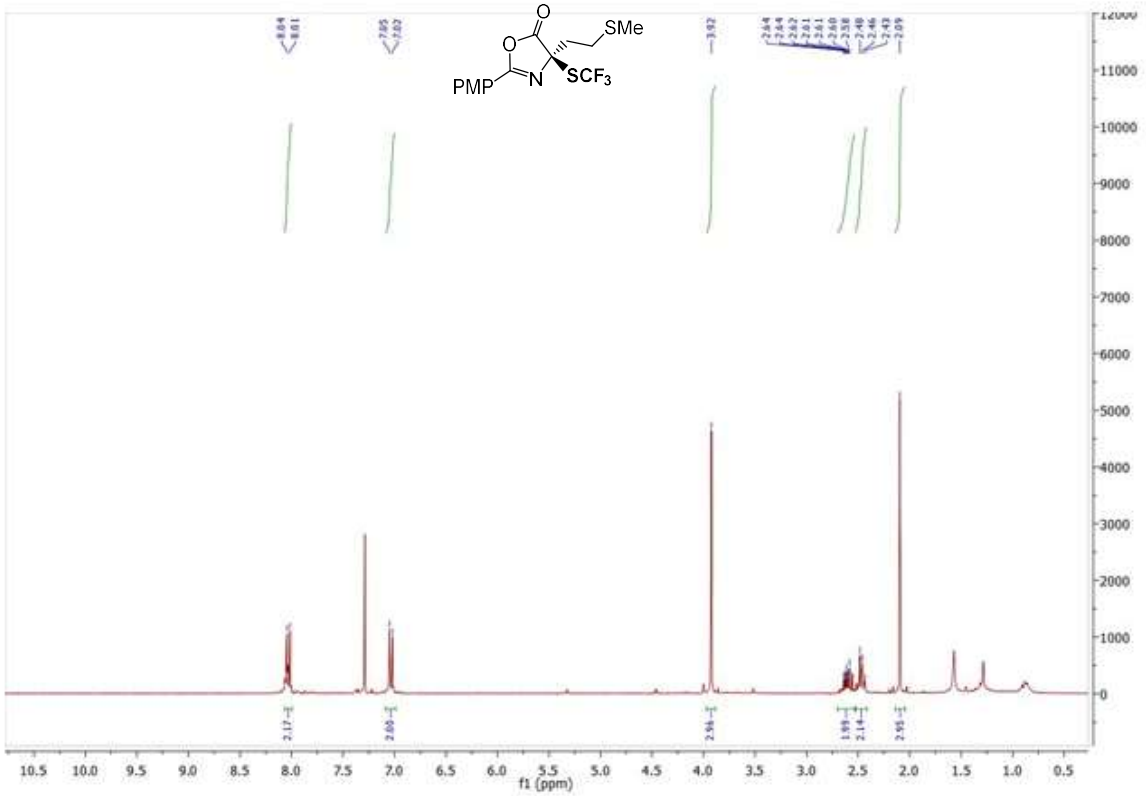

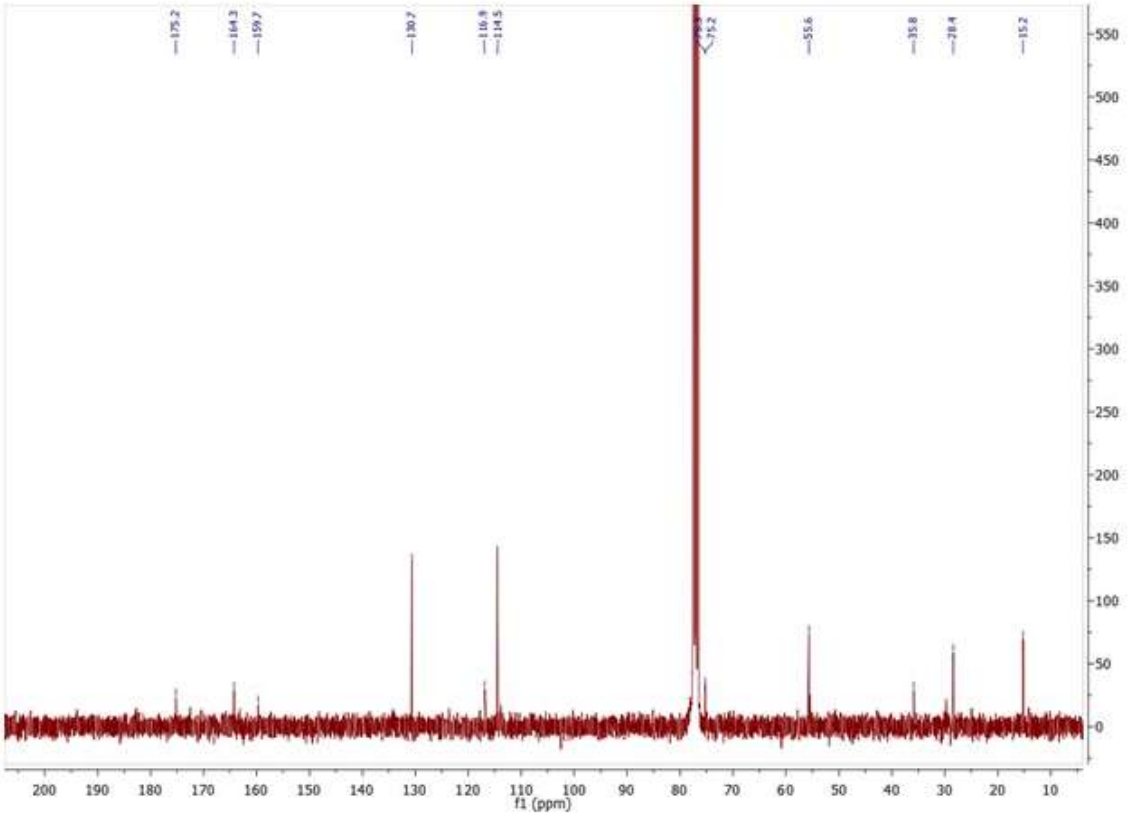
175.2
164.3
159.7
130.7
116.9
114.5
75.2
55.6
35.8
28.4
15.2
f1 (ppm)

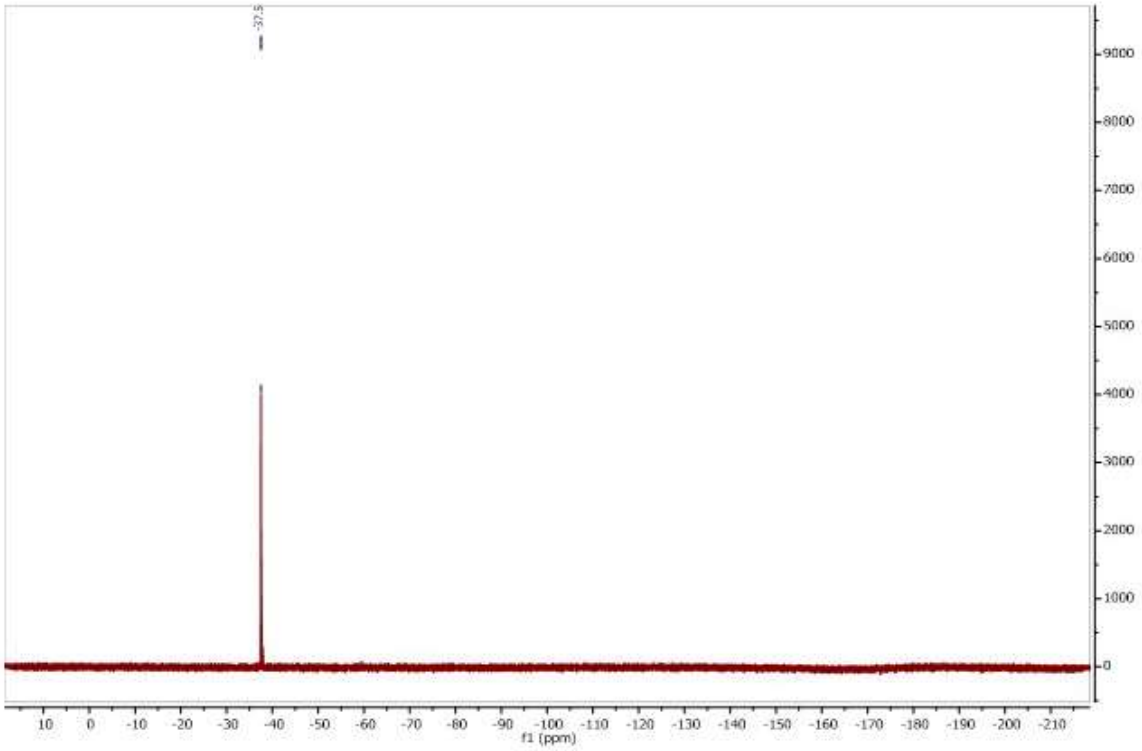
37.5
f1 (ppm)

4-(cyclohexylmethyl)-2-(4-methoxyphenyl)-4-((trifluoromethyl)thio)oxazol-5(4H)-one (3m)

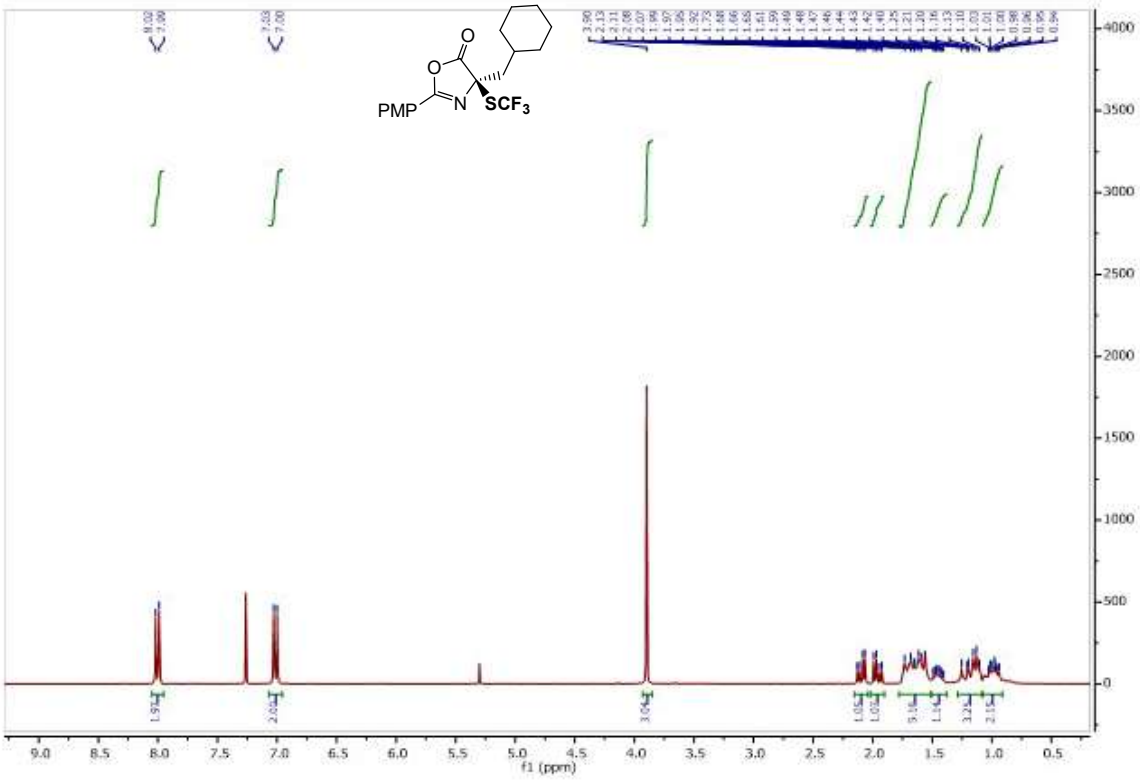

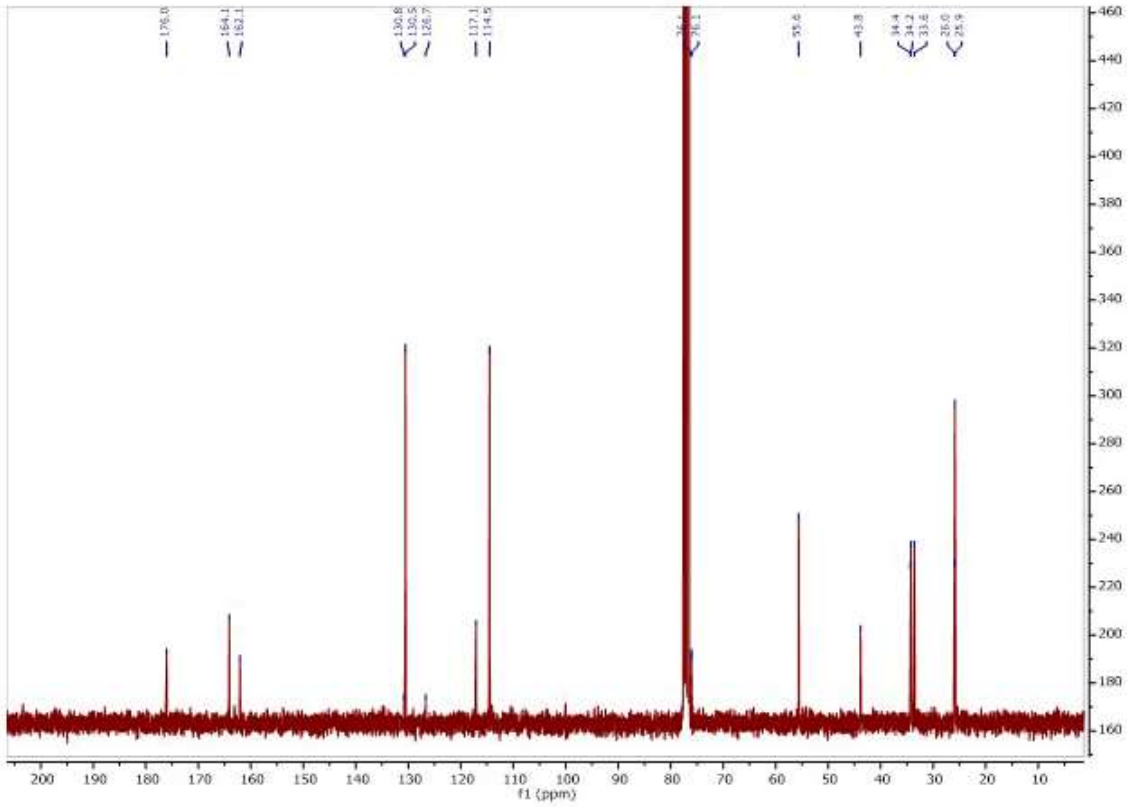

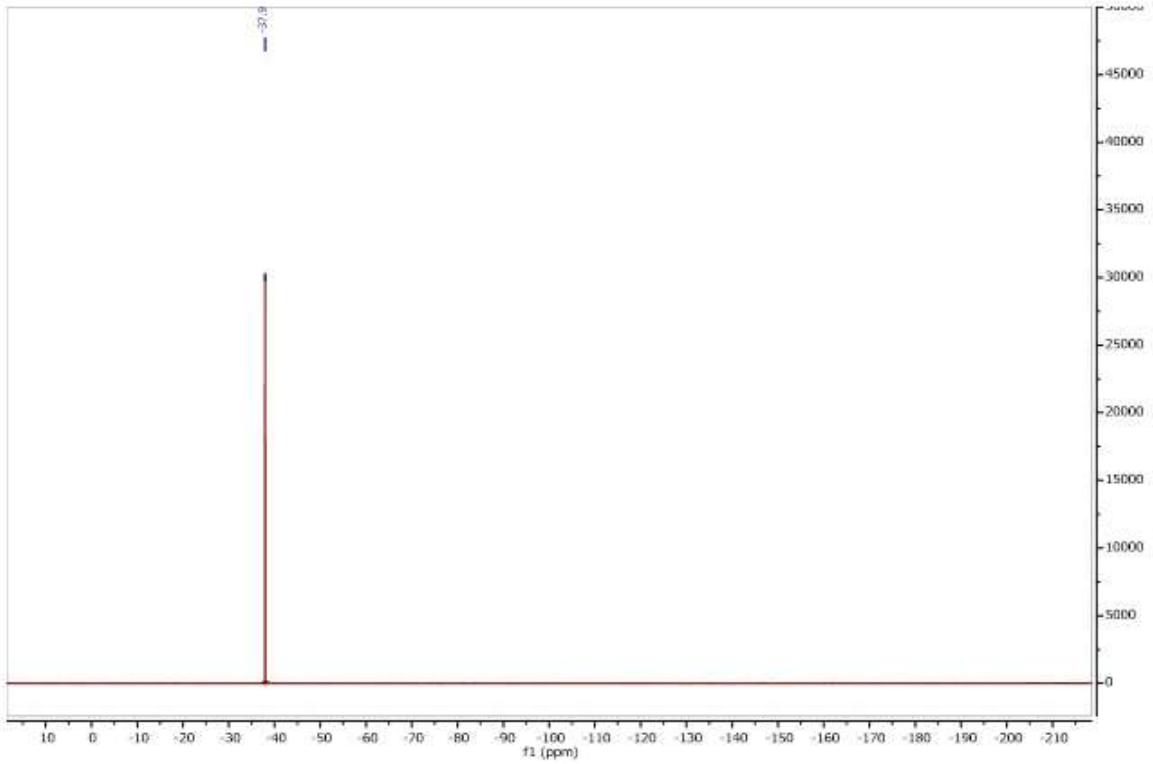

4-isobutyl-2-(4-methoxyphenyl)-4-((trifluoromethyl)thio)oxazol-5(4*H*)-one (3n)

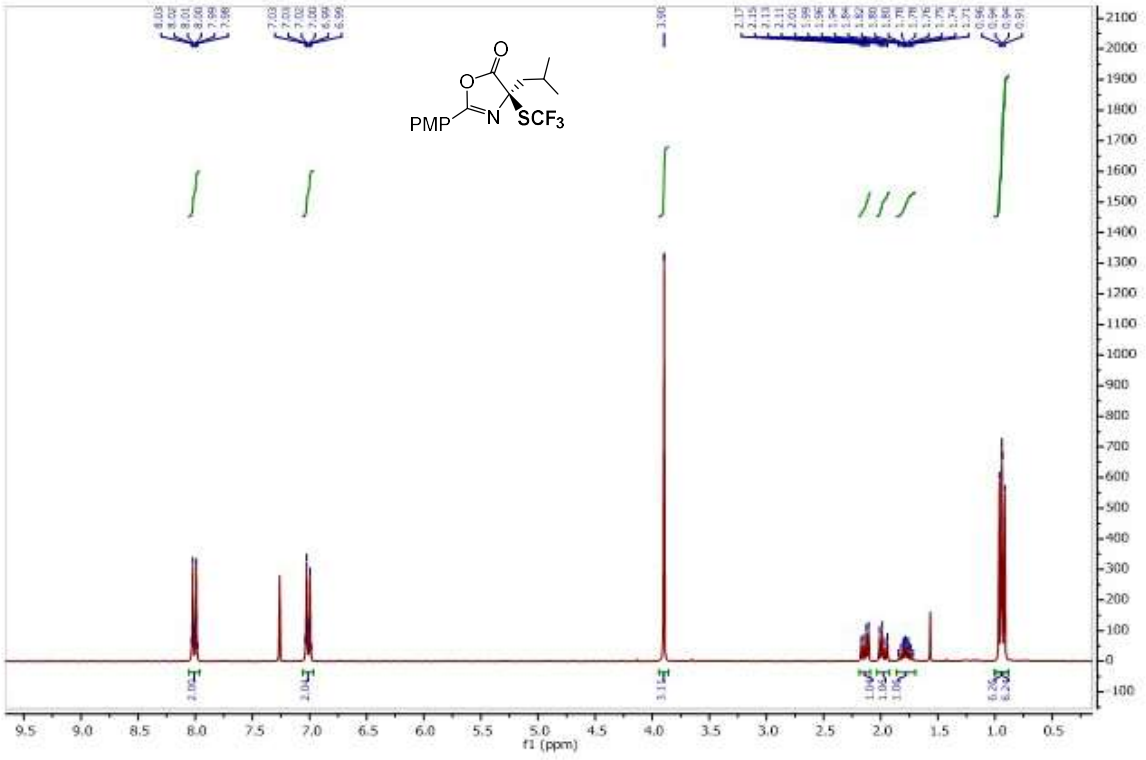

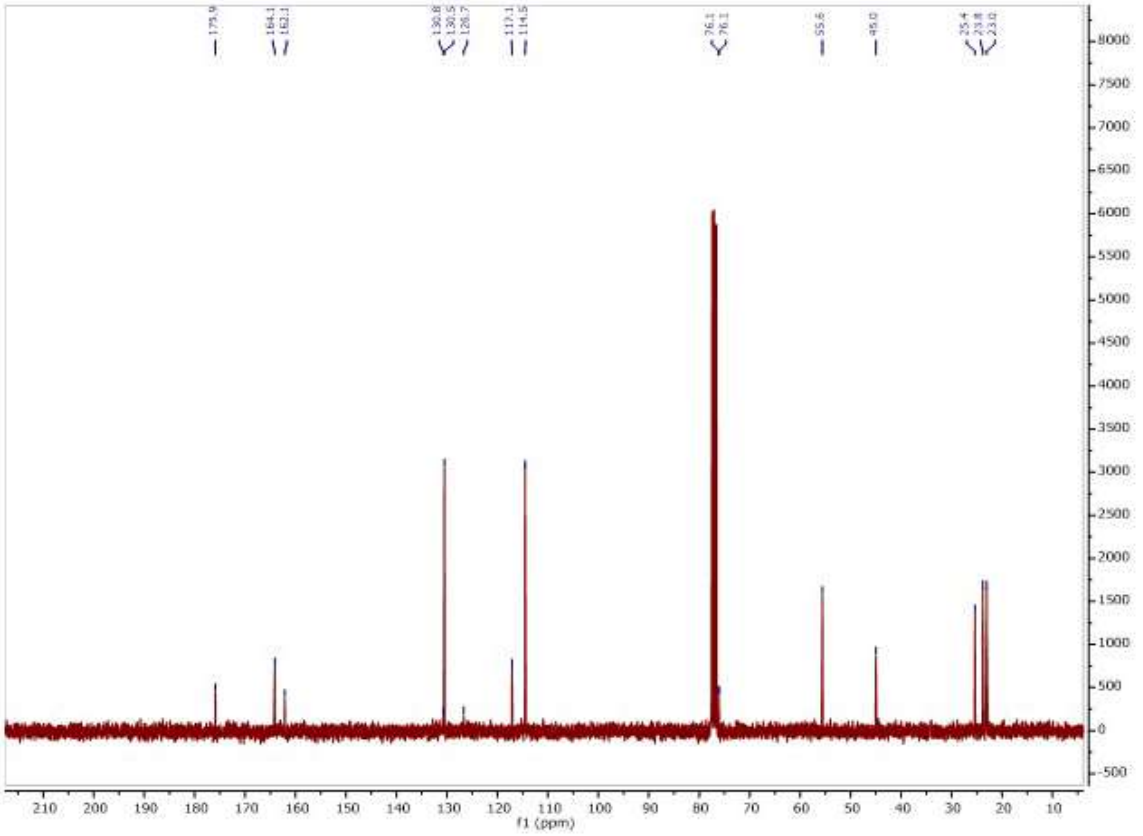
175.9
164.1
162.1
130.8
130.5
126.7
117.1
114.5
76.1
76.1
55.6
45.0
25.4
23.8
23.0
f1 (ppm)

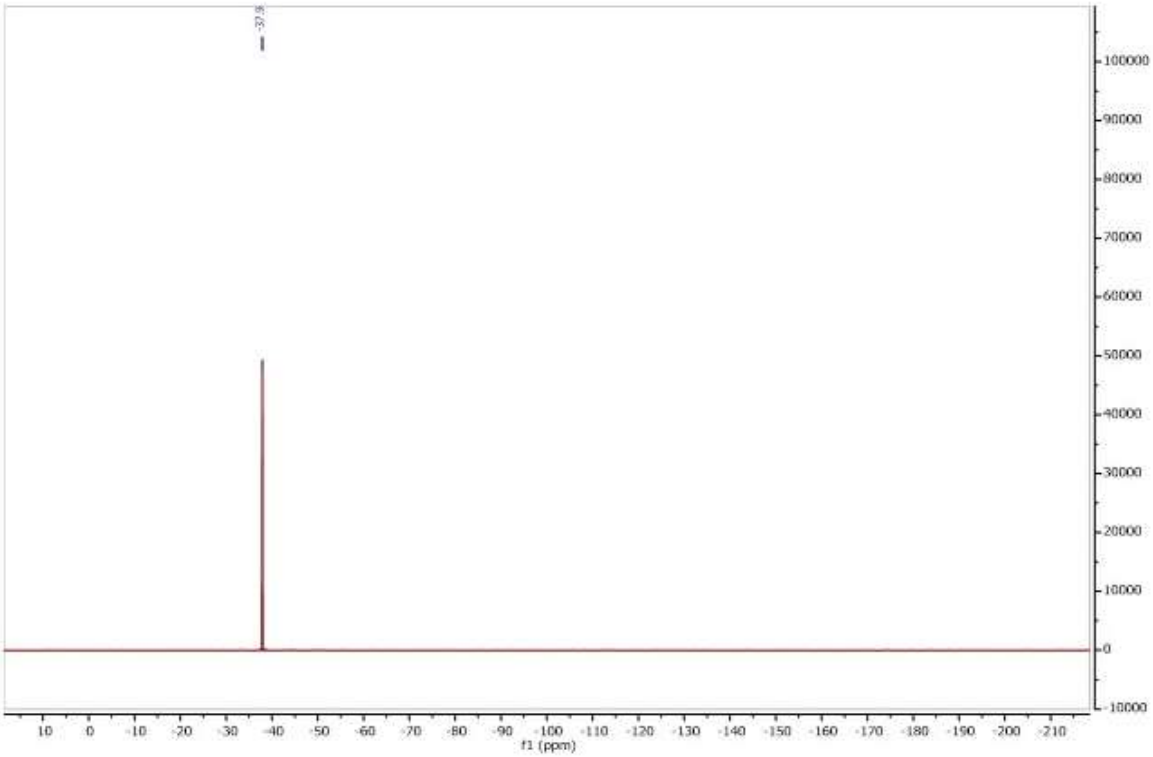
-37.8
f1 (ppm)

4-isopropyl-2-(4-methoxyphenyl)-4-((trifluoromethyl)thio)oxazol-5(4*H*)-one (3o)

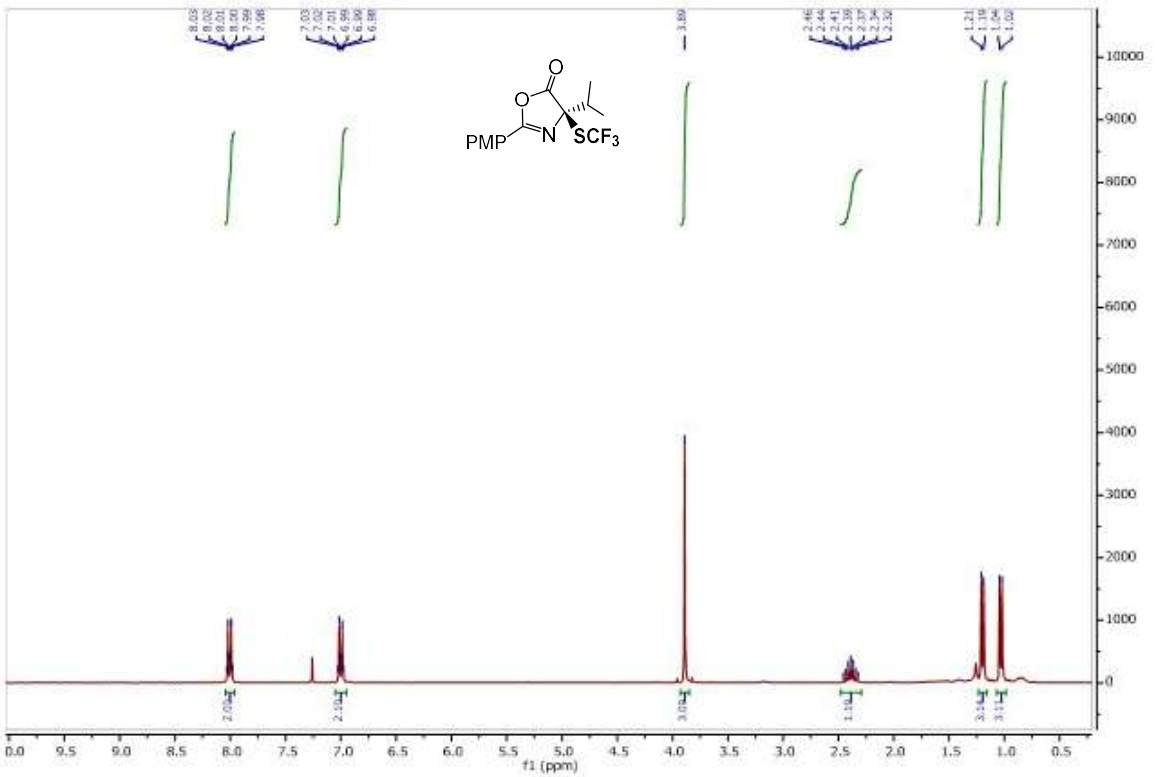

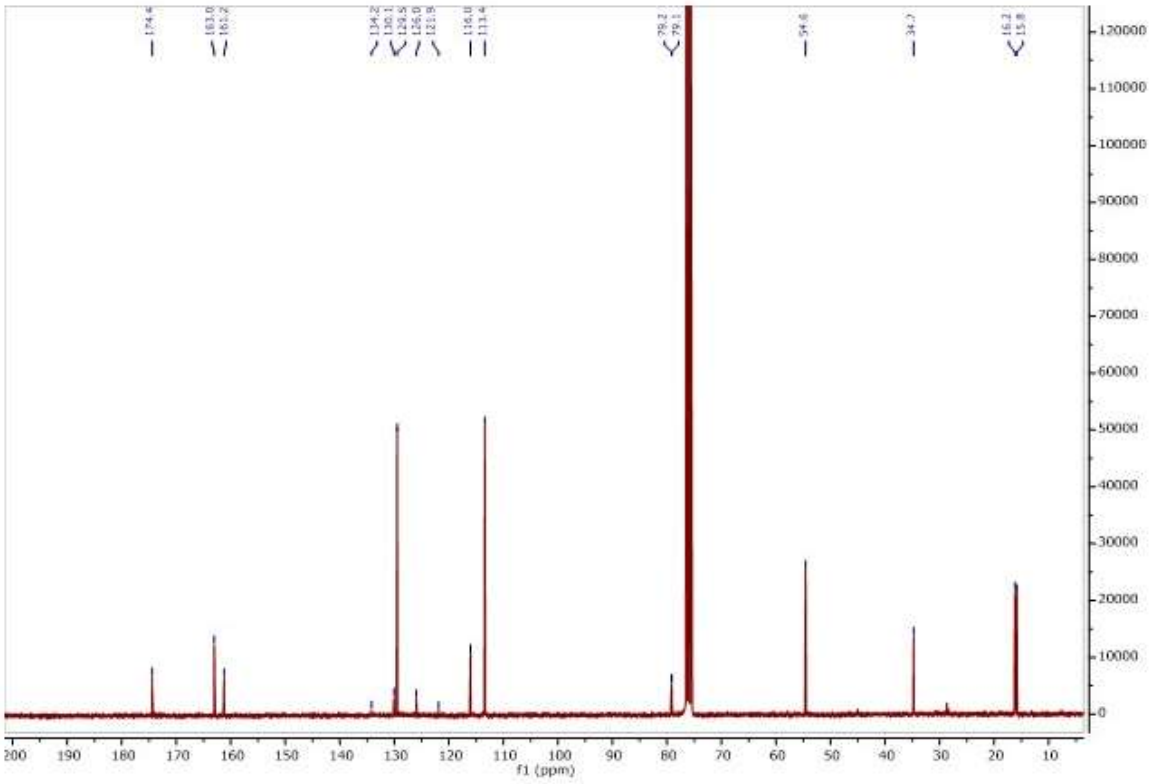

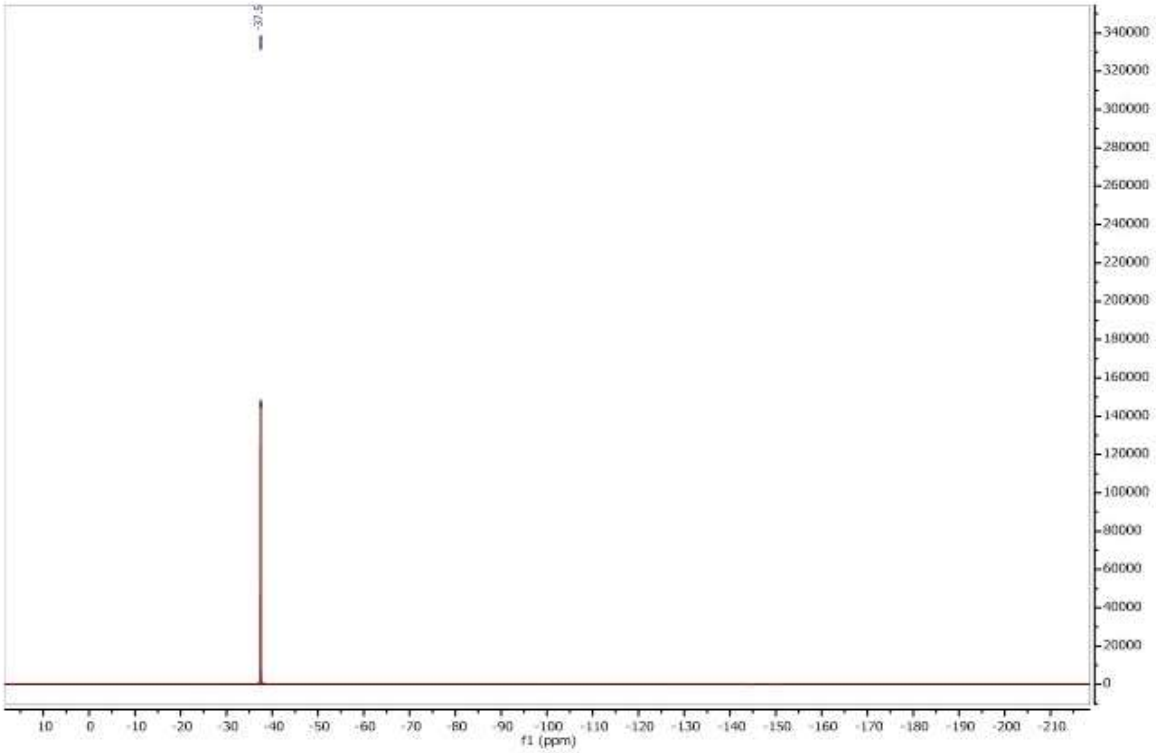

4-benzyl-2-phenyl-4-((trifluoromethyl)thio)oxazol-5(4*H*)-one (3a)

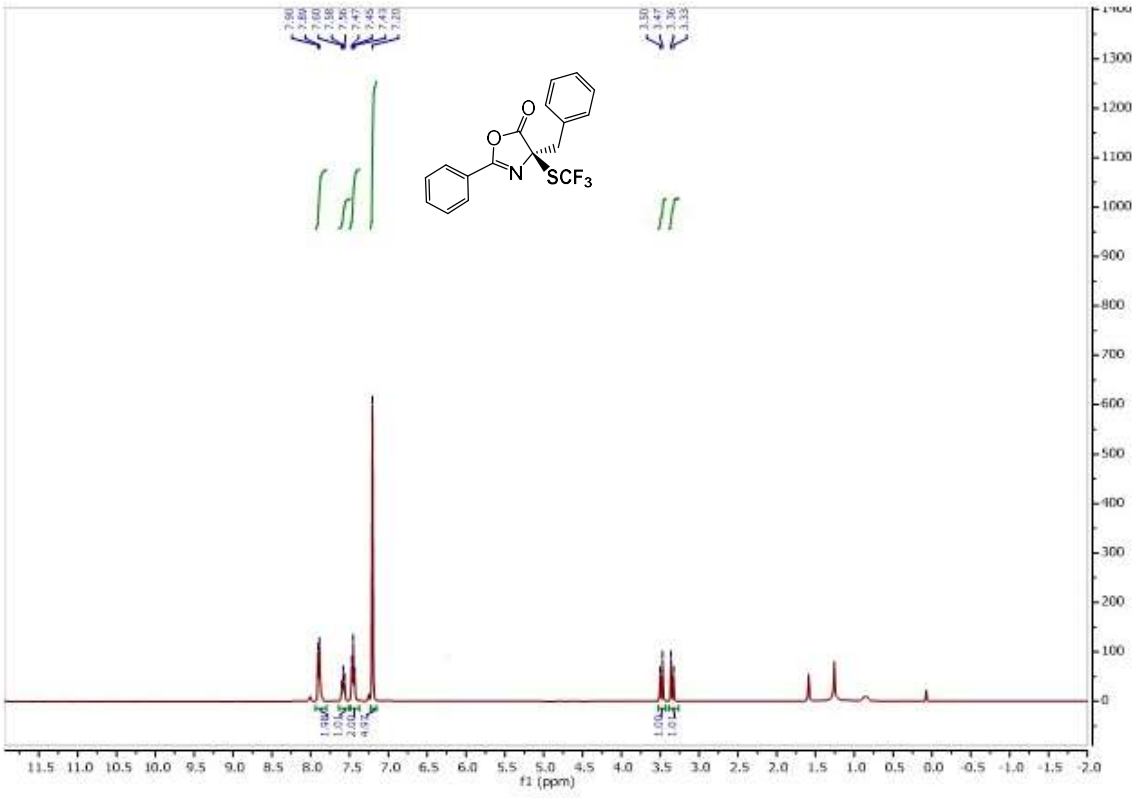

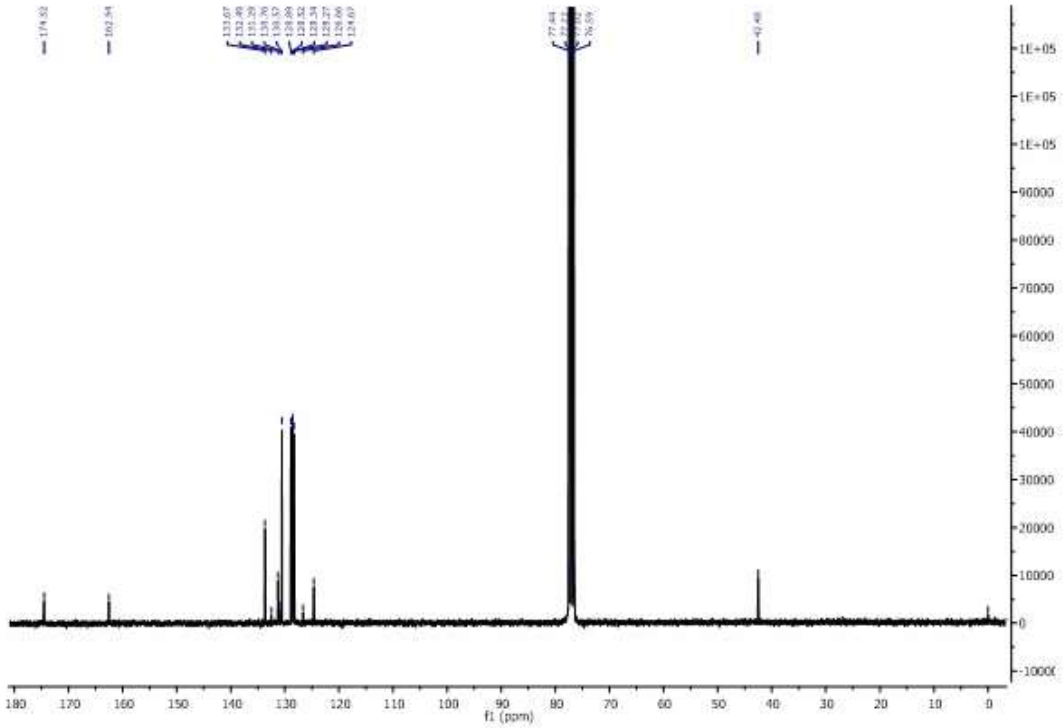
f1 (ppm)

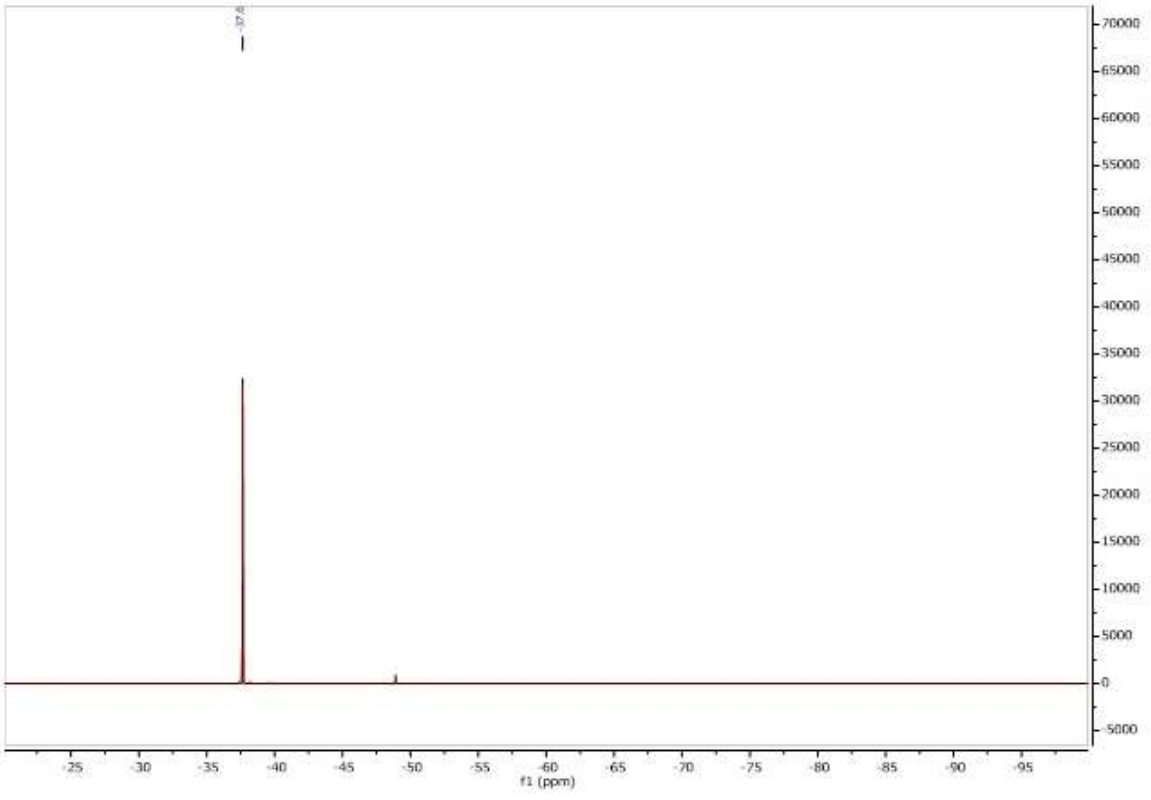
f1 (ppm)

4-benzyl-2-(4-chlorophenyl)-4-((trifluoromethyl)thio)oxazol-5(4*H*)-one (3d)

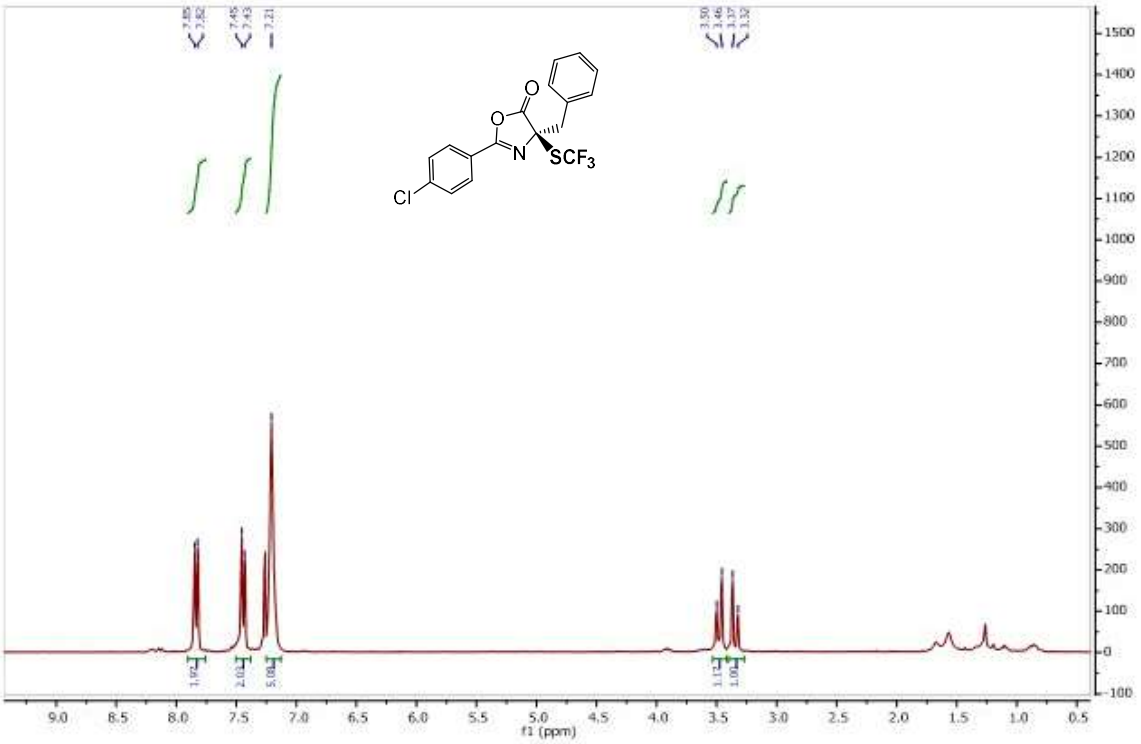

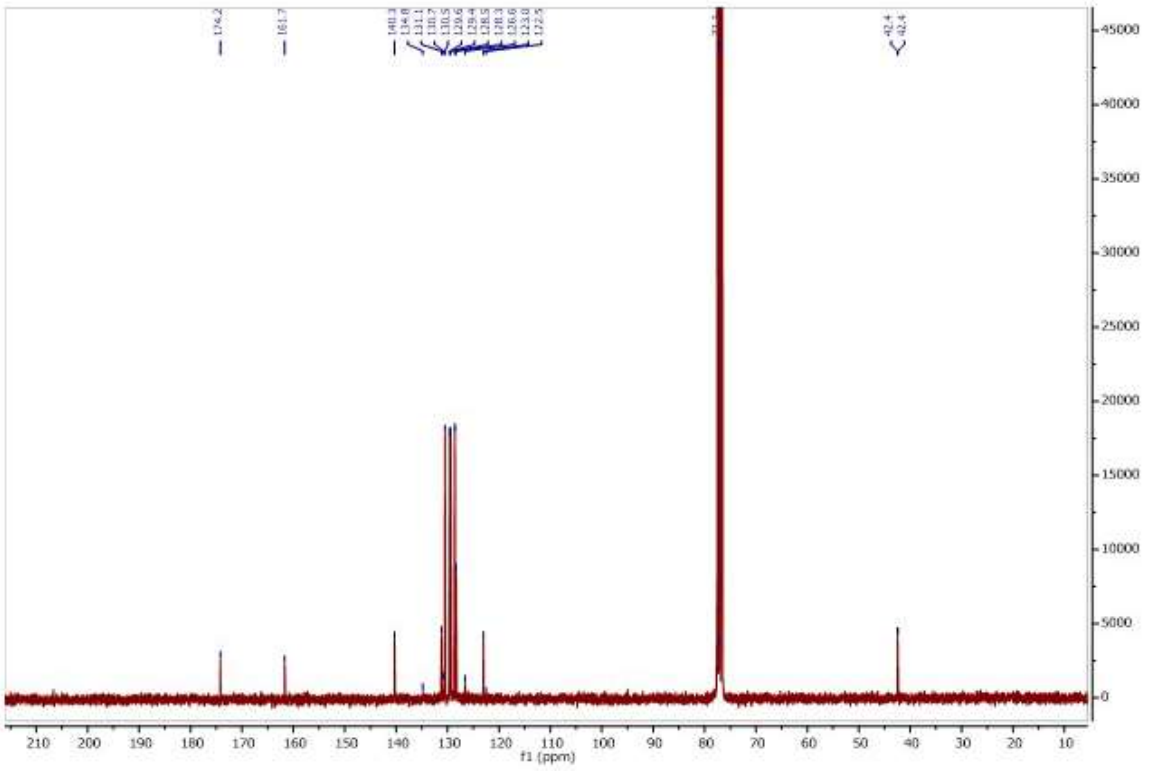

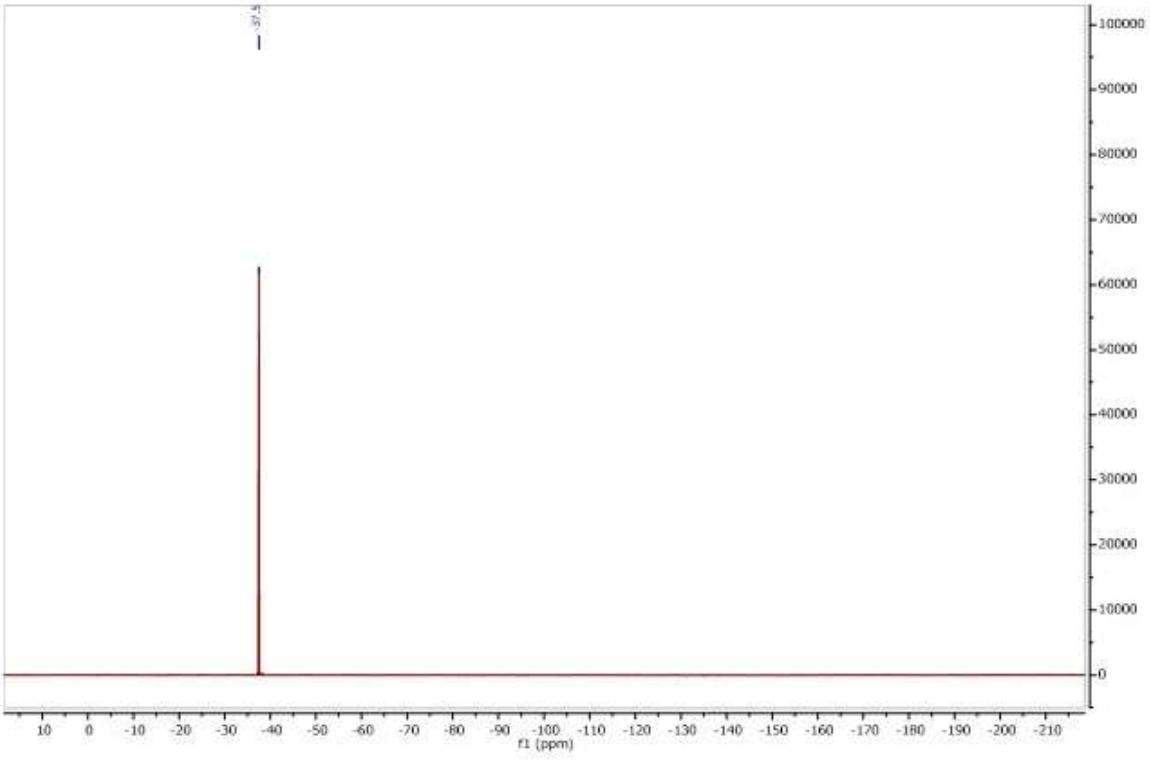
-37.5
100000
90000
80000
70000
60000
50000
40000
30000
20000
10000
0
10 0 -10 -20 -30 -40 -50 -60 -70 -80 -90 -100 -110 -120 -130 -140 -150 -160 -170 -180 -190 -200 -210
f1 (ppm)

Copies of chromatograms

Compound 3e

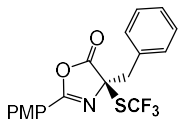

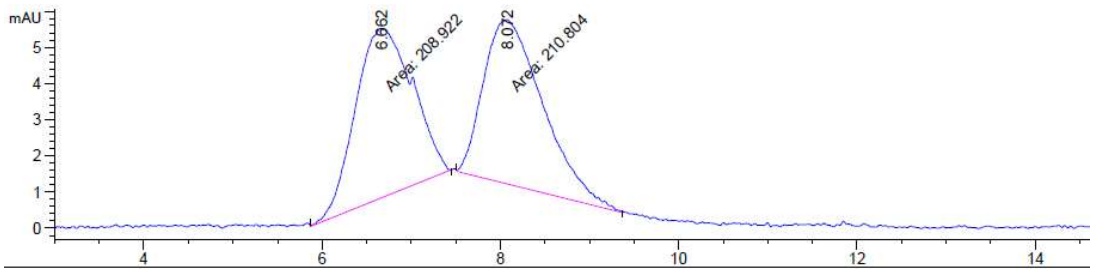

Signal 4: DAD1 D, Sig=280,4 Ref=360,100

Peak #	RetTime [min]	Type	Width [min]	Area [mAU*s]	Height [mAU]	Area %
1	6.662	MM	0.7416	208.92213	4.69559	49.7759
2	8.072	MM	0.7727	210.80374	4.54689	50.2241
Totals :				419.72588	9.24248	

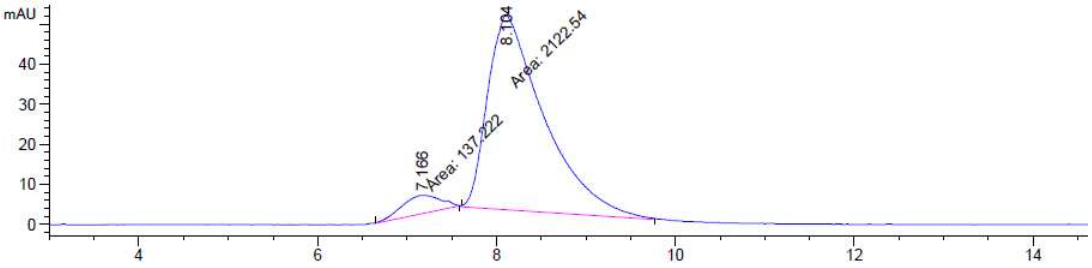

Signal 4: DAD1 D, Sig=280,4 Ref=360,100

Peak #	RetTime [min]	Type	Width [min]	Area [mAU*s]	Height [mAU]	Area %
1	7.166	MM	0.4993	137.22189	4.58037	6.0724
2	8.104	MM	0.7306	2122.53687	48.41775	93.9276

Compound 3f

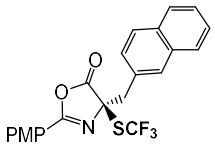

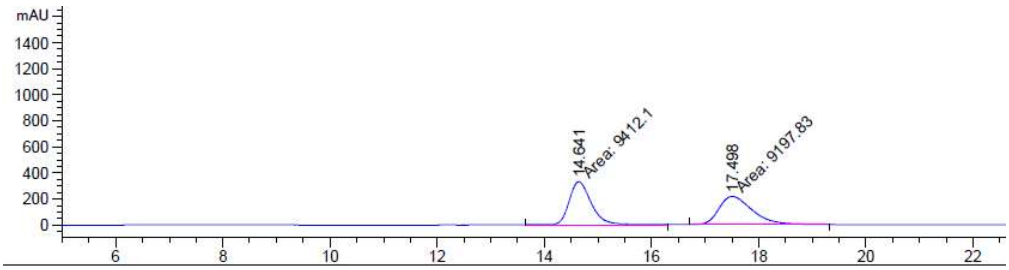

Signal 1: DAD1 A, Sig=254,4 Ref=360,100

Peak #	RetTime [min]	Type	Width [min]	Area [mAU*s]	Height [mAU]	Area %
1	14.641	MM	0.4771	9412.09570	328.78799	50.5757
2	17.498	MM	0.7142	9197.83203	214.62708	49.4243
Totals :				1.86099e4	543.41507	

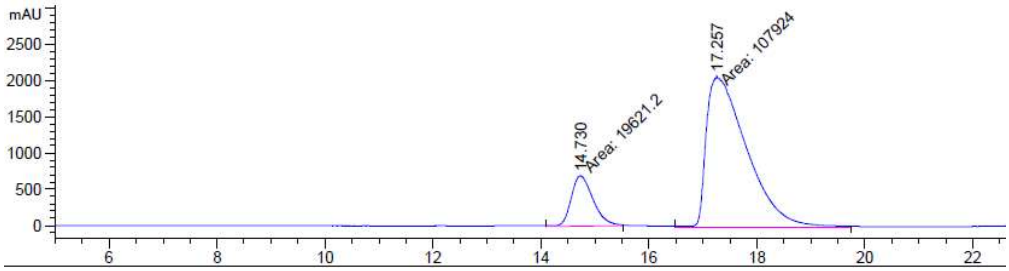

Signal 1: DAD1 A, Sig=254,4 Ref=360,100

Peak #	RetTime [min]	Type	Width [min]	Area [mAU*s]	Height [mAU]	Area %
1	14.730	MM	0.4720	1.96212e4	692.78754	15.3838
2	17.257	MM	0.8618	1.07924e5	2087.05786	84.6162
Totals :				1.27545e5	2779.84540	

Compound 3g

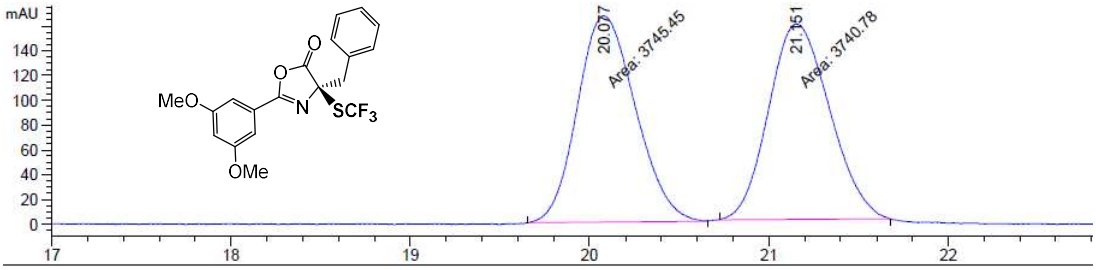

Signal 1: DAD1 A, Sig=254,4 Ref=360,100

Peak #	RetTime [min]	Type	Width [min]	Area [mAU*s]	Height [mAU]	Area %
1	20.077	MM	0.3750	3745.44946	166.44315	50.0312
2	21.151	MM	0.3947	3740.78394	157.94070	49.9688
Totals :				7486.23340	324.38385	

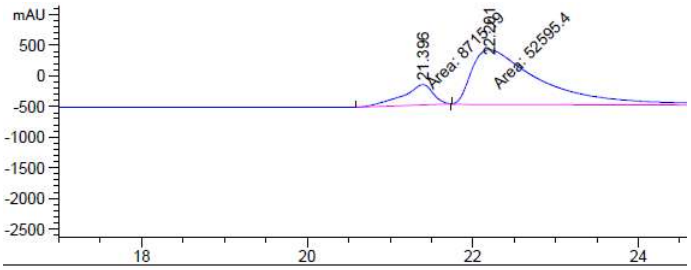

Signal 1: DAD1 A, Sig=254,4 Ref=360,100

Peak #	RetTime [min]	Type	Width [min]	Area [mAU*s]	Height [mAU]	Area %
1	21.396	MM	0.4339	8715.18750	334.76059	14.2148
2	22.201	MM	0.9813	5.25954e4	893.33795	85.7852
Totals :				6.13105e4	1228.09854	

Compound 3h

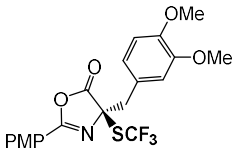

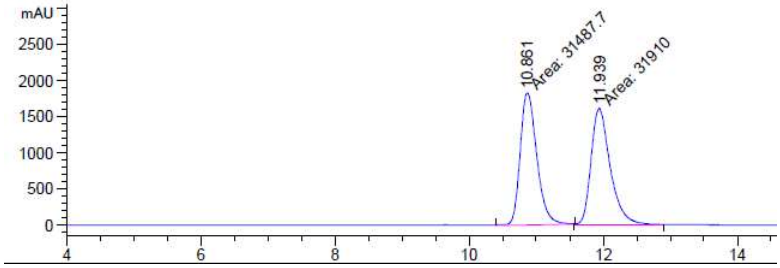

Signal 1: DAD1 A, Sig=254,4 Ref=360,100

Peak #	RetTime [min]	Type	Width [min]	Area [mAU*s]	Height [mAU]	Area %
1	10.861	MM	0.2873	3.14877e4	1826.38391	49.6669
2	11.939	MM	0.3305	3.19100e4	1609.41138	50.3331
Totals :				6.33978e4	3435.79529	

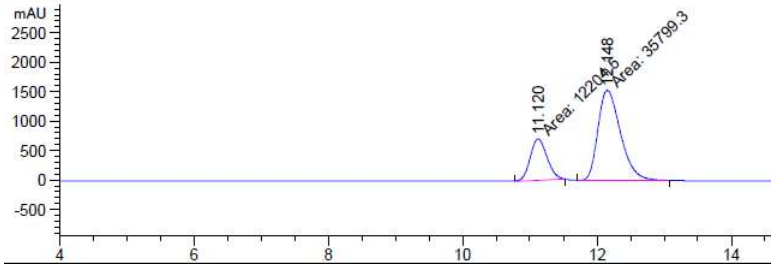

Signal 1: DAD1 A, Sig=254,4 Ref=360,100

Peak #	RetTime [min]	Type	Width [min]	Area [mAU*s]	Height [mAU]	Area %
1	11.120	MM	0.2895	1.22045e4	702.67035	25.4240
2	12.148	MM	0.3896	3.57993e4	1531.41418	74.5760
Totals :				4.80038e4	2234.08453	

Compound 3i

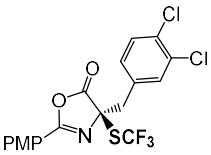

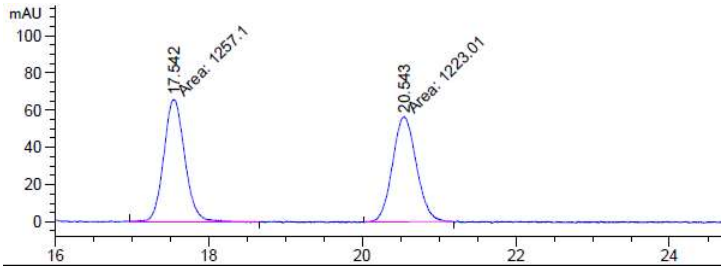

Signal 1: DAD1 A, Sig=254,4 Ref=360,100

Peak #	RetTime [min]	Type	Width [min]	Area [mAU*s]	Height [mAU]	Area %
1	17.542	MM	0.3183	1257.09802	65.83231	50.6873
2	20.543	MM	0.3611	1223.00745	56.45263	49.3127
Totals :				2480.10547	122.28493	

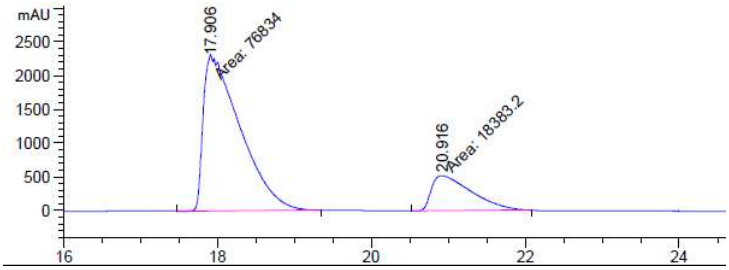

Signal 1: DAD1 A, Sig=254,4 Ref=360,100

Peak #	RetTime [min]	Type	Width [min]	Area [mAU*s]	Height [mAU]	Area %
1	17.906	MM	0.5558	7.68340e4	2304.09839	80.6934
2	20.916	MM	0.5945	1.83832e4	515.37238	19.3066
Totals :				9.52172e4	2819.47076	

Compound 3j

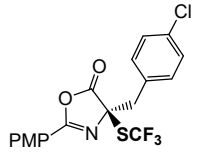

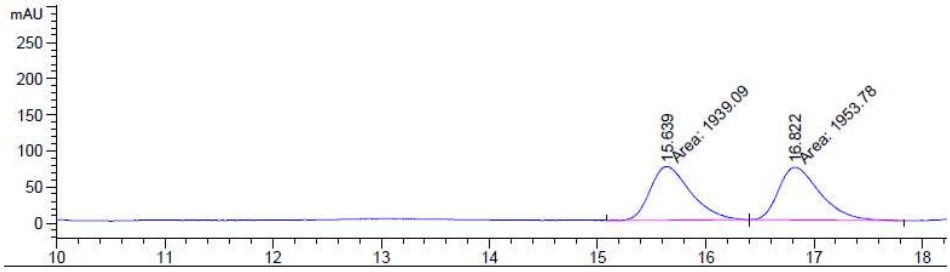

Signal 1: DAD1 A, Sig=254,4 Ref=360,100

Peak #	RetTime [min]	Type	Width [min]	Area [mAU*s]	Height [mAU]	Area %
1	15.639	MM	0.4344	1939.09045	74.39991	49.8113
2	16.822	MM	0.4453	1953.77966	73.13407	50.1887
Totals :				3892.87012	147.53398	

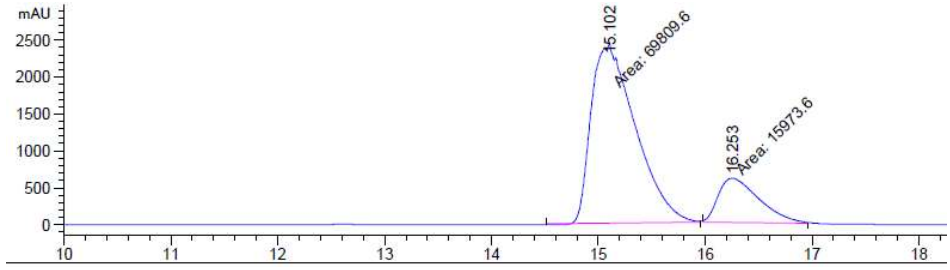

Signal 1: DAD1 A, Sig=254,4 Ref=360,100

Peak #	RetTime [min]	Type	Width [min]	Area [mAU*s]	Height [mAU]	Area %
1	15.102	MM	0.4789	6.98096e4	2429.45972	81.3792
2	16.253	MM	0.4434	1.59736e4	600.45313	18.6208
Totals :				8.57832e4	3029.91284	

Compound 3k

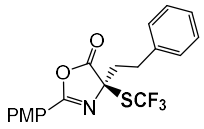

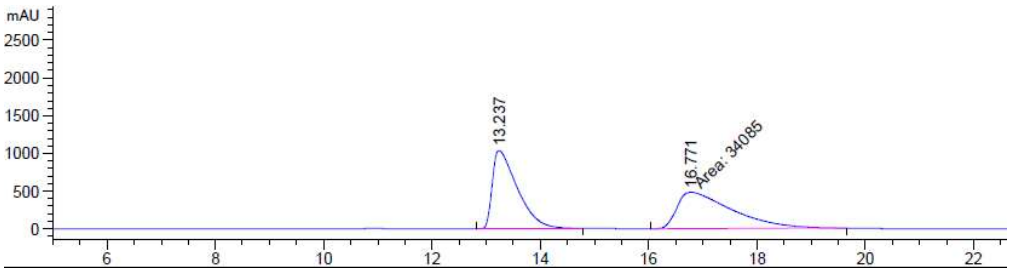

Signal 1: DAD1 A, Sig=254,4 Ref=360,100

Peak #	RetTime [min]	Type	Width [min]	Area [mAU*s]	Height [mAU]	Area %
1	13.237	VV	0.4260	3.36488e4	1038.55286	49.6780
2	16.771	MM	1.1794	3.40850e4	481.66440	50.3220
Totals :				6.77338e4	1520.21725	

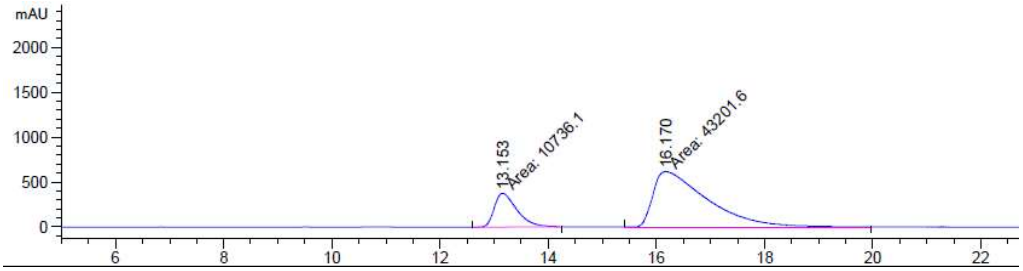

Signal 1: DAD1 A, Sig=254,4 Ref=360,100

Peak #	RetTime [min]	Type	Width [min]	Area [mAU*s]	Height [mAU]	Area %
1	13.153	MM	0.4782	1.07361e4	374.15536	19.9047
2	16.170	MM	1.1661	4.32016e4	617.44269	80.0953
Totals :				5.39377e4	991.59805	

Compound 3l

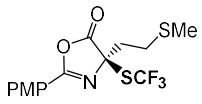

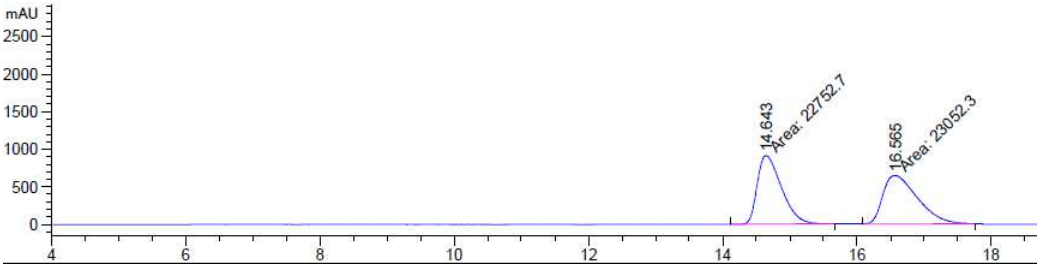

Signal 1: DAD1 A, Sig=254,4 Ref=360,100

Peak #	RetTime [min]	Type	Width [min]	Area [mAU*s]	Height [mAU]	Area %
1	14.643	MM	0.4165	2.27527e4	910.36652	49.6730
2	16.565	MM	0.5954	2.30523e4	645.27203	50.3270
Totals :				4.58050e4	1555.63855	

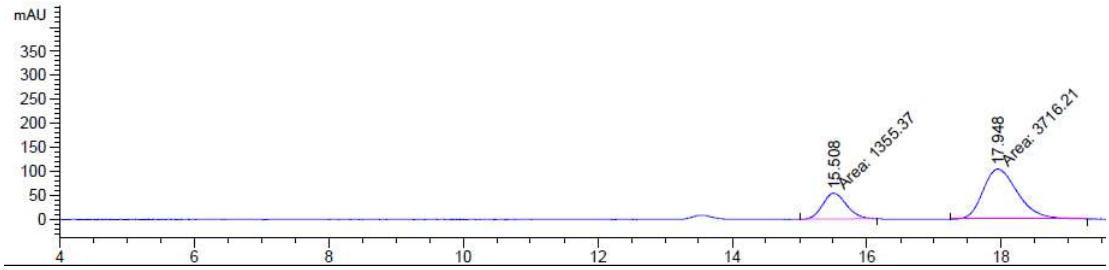

Signal 1: DAD1 A, Sig=254,4 Ref=360,100

Peak #	RetTime [min]	Type	Width [min]	Area [mAU*s]	Height [mAU]	Area %
1	15.508	MM	0.4190	1355.36768	53.90687	26.7248
2	17.948	MM	0.5975	3716.20532	103.65303	73.2752
Totals :				5071.57300	157.55990	

Compound 3m

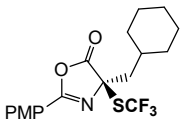

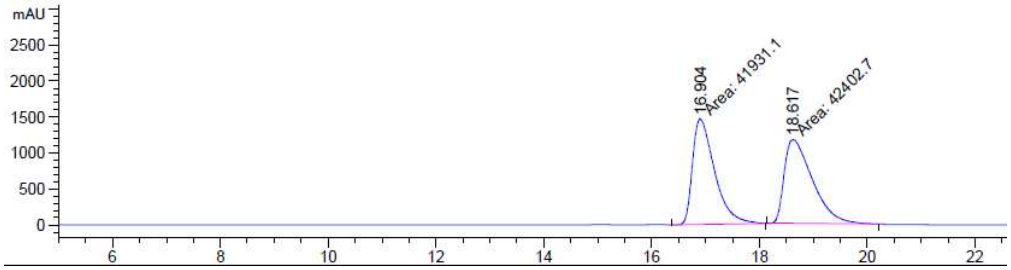

Signal 1: DAD1 A, Sig=254,4 Ref=360,100

Peak #	RetTime [min]	Type	Width [min]	Area [mAU*s]	Height [mAU]	Area %
1	16.904	MM	0.4760	4.19311e4	1468.31055	49.7204
2	18.617	MM	0.6081	4.24027e4	1162.21411	50.2796
Totals :				8.43339e4	2630.52466	

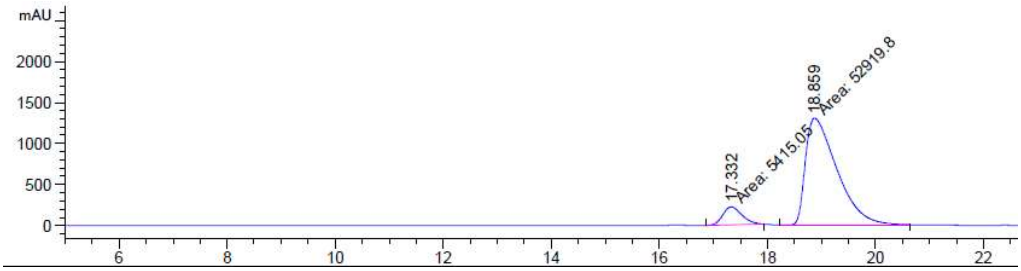

Signal 1: DAD1 A, Sig=254,4 Ref=360,100

Peak #	RetTime [min]	Type	Width [min]	Area [mAU*s]	Height [mAU]	Area %
1	17.332	MM	0.4112	5415.05078	219.50145	9.2827
2	18.859	MM	0.6785	5.29198e4	1299.93848	90.7173
Totals :				5.83348e4	1519.43993	

Compound 3n

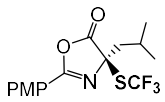

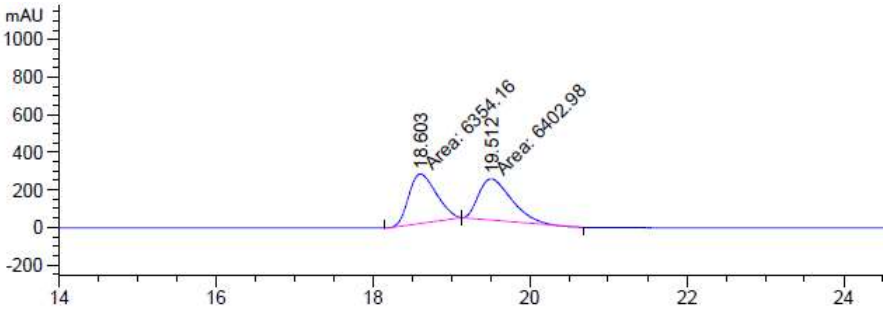

Signal 1: DAD1 A, Sig=254,4 Ref=360,100

Peak #	RetTime [min]	Type	Width [min]	Area [mAU*s]	Height [mAU]	Area %
1	18.603	MM	0.4043	6354.16064	261.97104	49.8087
2	19.512	MM	0.4875	6402.97900	218.90417	50.1913
Totals :				1.27571e4	480.87521	

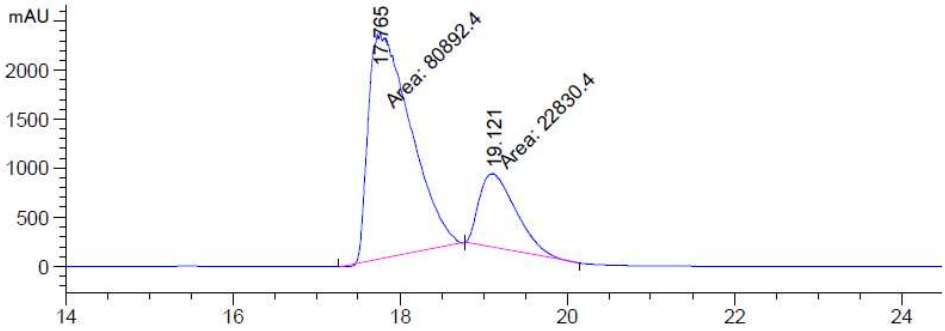

Signal 1: DAD1 A, Sig=254,4 Ref=360,100

Peak #	RetTime [min]	Type	Width [min]	Area [mAU*s]	Height [mAU]	Area %
1	17.765	MM	0.5820	8.08924e4	2316.66431	77.9890
2	19.121	MM	0.5095	2.28304e4	746.82599	22.0110
Totals :				1.03723e5	3063.49030	

Compound 3o

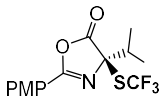

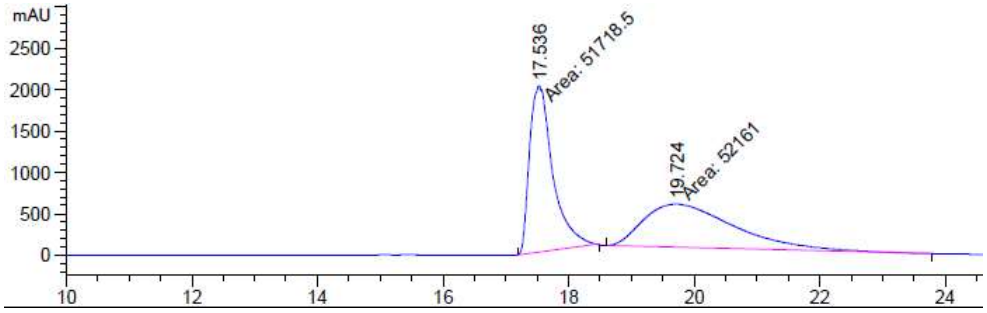

Signal 1: DAD1 A, Sig=254,4 Ref=360,100

Peak #	RetTime [min]	Type	Width [min]	Area [mAU*s]	Height [mAU]	Area %
1	17.536	MM	0.4287	5.17185e4	2010.45935	49.7870
2	19.724	MM	1.6709	5.21610e4	520.29285	50.2130
Totals :				1.03879e5	2530.75220	

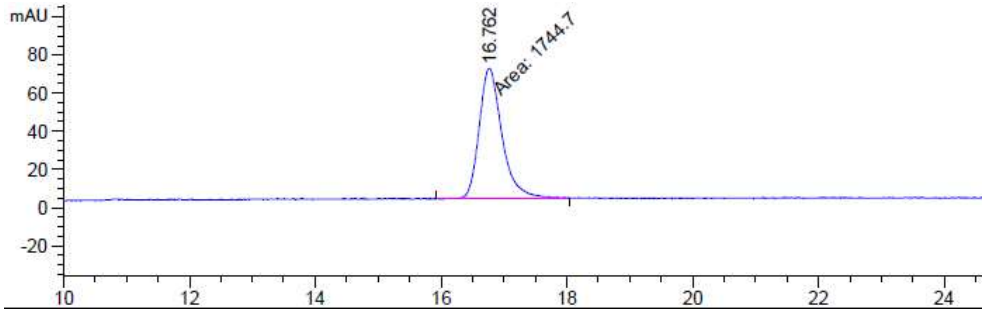

Signal 1: DAD1 A, Sig=254,4 Ref=360,100

Peak #	RetTime [min]	Type	Width [min]	Area [mAU*s]	Height [mAU]	Area %
1	16.762	MM	0.4255	1744.70483	68.34391	100.0000
Totals :				1744.70483	68.34391	

Compound 3a

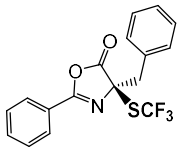

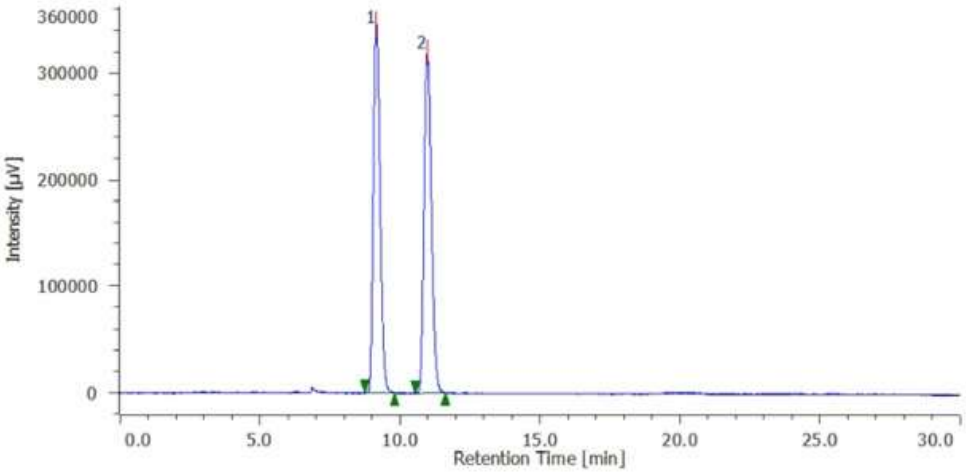

#	Peak Name	CH	tR [min]	Area [μV·sec]	Height [μV]	Area%	Height%	Quantity	NTP	Resolution	Symmetry Factor	Warning
1	Unknown	10	9.150	5723324	345713	49.481	52.014	N/A	6943	3.951	1.267	
2	Unknown	10	10.974	5843411	318946	50.519	47.986	N/A	8144	N/A	1.208	

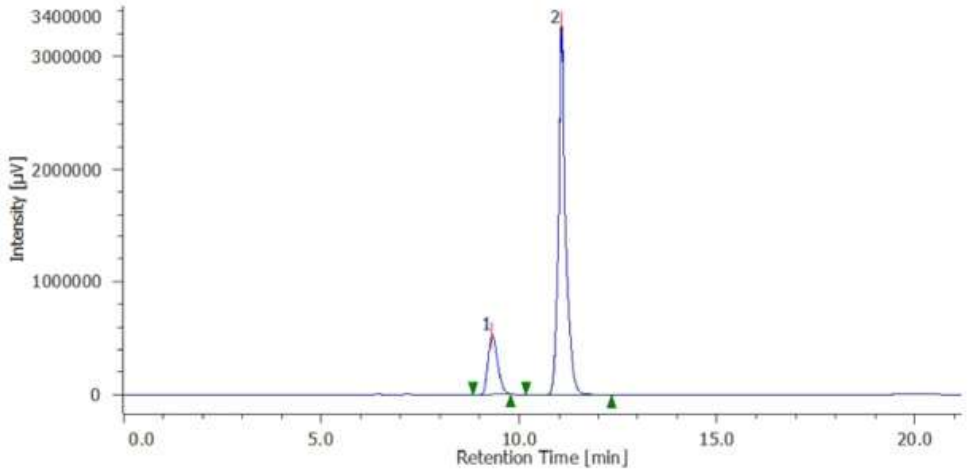

#	Peak Name	CH	tR [min]	Area [μV·sec]	Height [μV]	Area%	Height%	Quantity	NTP	Resolution	Symmetry Factor	Warning
1	Unknown	9	9.313	8908785	525720	17.655	13.796	N/A	6824	4.931	1.292	
2	Unknown	9	11.066	41552503	3284902	82.345	86.204	N/A	28592	N/A	1.276	

Compound 3d

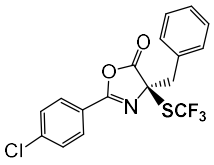

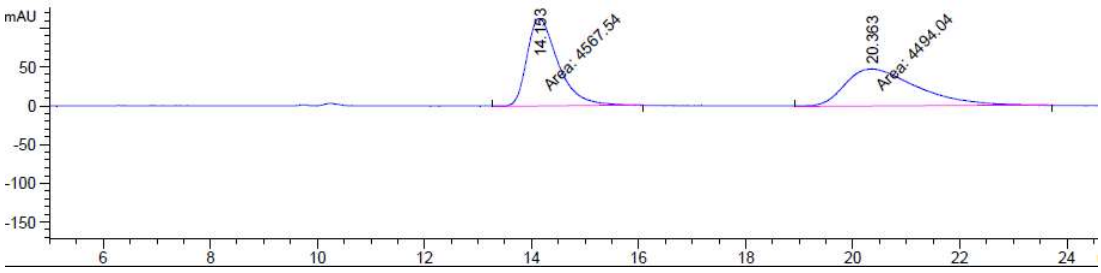

Signal 1: DAD1 A, Sig=254,4 Ref=360,100

Peak #	RetTime [min]	Type	Width [min]	Area [mAU*s]	Height [mAU]	Area %
1	14.153	MM	0.6748	4567.53711	112.80434	50.4055
2	20.363	MM	1.5635	4494.04297	47.90648	49.5945
Totals :				9061.58008	160.71082	

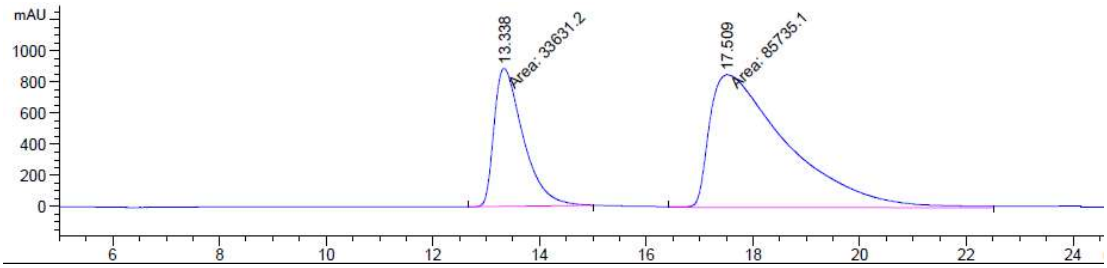

Signal 1: DAD1 A, Sig=254,4 Ref=360,100

Peak #	RetTime [min]	Type	Width [min]	Area [mAU*s]	Height [mAU]	Area %
1	13.338	MM	0.6323	3.36312e4	886.43542	28.1748
2	17.509	MM	1.6781	8.57351e4	851.51392	71.8252
Totals :				1.19366e5	1737.94934	